NASA TECHNICAL NOTE

NASA TN D-7912

NASA TN D-7912

COMPARATIVE EVALUATION OF TEST METHODS TO SIMULATE ACOUSTIC RESPONSE OF SHROUD-ENCLOSED SPACECRAFT STRUCTURES

Frank J. On

Goddard Space Flight Center
Greenbelt, Md. 20771

NATIONAL AERONAUTICS AND SPACE ADMINISTRATION • WASHINGTON, D. C. • MARCH 1975

1. Report No.	2. Government Accession No.	3. Recipient's Catalog No.
NASA TN D-7912		

4. Title and Subtitle	5. Report Date
Comparative Evaluation of Test Methods to Simulate Acoustic Response of Shroud-enclosed Spacecraft Structures	March 1975
	6. Performing Organization Code 321
7. Author(s) Frank J. On	8. Performing Organization Report No. G-7553
9. Performing Organization Name and Address Goddard Space Flight Center Greenbelt, Maryland 20771	10. Work Unit No. 502-22-11-01
	11. Contract or Grant No.
	13. Type of Report and Period Covered Technical Note
12. Sponsoring Agency Name and Address National Aeronautics and Space Administration Washington, D. C. 20546	14. Sponsoring Agency Code

15. Supplementary Notes

16. Abstract

A comparative evaluation was made of test methods, to ascertain whether a spacecraft, properly tested within its shroud, could be vibroacoustic tested without the shroud, with adjustments made in the acoustic input spectra to simulate the acoustic response of the missing shroud. The evaluation was based primarily on vibroacoustic test results obtained first from a baseline model composed of a spacecraft with adapter, lower support structure, and shroud; second, of the spacecraft, adapter, and lower structure, but without the shroud; and third, of the spacecraft and adapter only. Emphasis was placed on (1) the magnitude of the acoustic input changes required to substitute for the shroud and the difficulty of making such input changes, and (2) the degree of missimulation which can result from the performance of a particular, less-than-optimum test. Conclusions are drawn with regard to the advantages and disadvantages derived from the use of input spectra adjustment methods and lower support structure simulations. Test guidelines are also developed for planning and performing a launch acoustic-environmental test.

17. Key Words (Selected by Author(s))	18. Distribution Statement
Structural mechanics; Acoustics; Simulation; Testing	Unclassified–Unlimited CAT. 18

19. Security Classif. (of this report)	20. Security Classif. (of this page)	21. No. of Pages	22. Price*
Unclassified	Unclassified	56	$4.25

*For sale by the National Technical Information Service, Springfield, Virginia 22151.

CONTENTS

ILLUSTRATIONS

ILLUSTRATIONS (continued)

ILLUSTRATIONS (continued)

ILLUSTRATIONS (continued)

TABLES

COMPARATIVE EVALUATION OF TEST METHODS TO SIMULATE ACOUSTIC RESPONSE OF SHROUD-ENCLOSED SPACECRAFT STRUCTURES

Frank J. On
Goddard Space Flight Center

SUMMARY

This report presents a comparative evaluation of test methods used to simulate the acoustic response of shroud-enclosed spacecraft structures. The evaluation was based on the vibro-acoustic test results obtained from a single baseline model of a spacecraft with adapter, lower support structure, and shroud. Emphasis was placed on investigating (1) the magnitude of and the difficulty of producing the test-input changes which would be required to generate the responses, in an acoustic test and random vibration test of a spacecraft and adapter only, which would be comparable to the responses produced by similar tests of the baseline model with the shroud installed; and (2) the degree of missimulation which can result from performance of a specified, less-than-optimum test.

The study shows that an acoustic test with the shroud removed, but with simulated internal acoustic inputs, cannot in general duplicate the responses that result with the shroud installed and both the spacecraft and shroud subjected to corresponding external, acoustic inputs. The adjustment of the input frequency-band levels to account for the absence of the shroud offers an effective approach only to the simulation of zonal response. The successful simulation of one zone cannot guarantee successful simulation at all zones. The indiscriminate use of a lower support structure, to compensate for the absence of a shroud, is cautioned against.

Single-axis, random vibration testing, when used to simulate the lateral and longitudinal responses which result from the acoustic testing of a shroud-installed spacecraft, has been found to be seriously limited in the high-frequency region and it is effective only in local zones.

Based on the results of this study, spacecraft test guidelines are developed which can be helpful in planning and performing environmental tests that are designed to simulate the effects of launch acoustic noise.

INTRODUCTION

Spacecraft test methods used to simulate the launch acoustic environment are most often in one of two forms. Either the spacecraft alone, without the shroud, is subjected to the

acoustic environment expected to occur within the shroud-spacecraft cavity, or the spacecraft is subjected to single-axis random vibration input at the base of the adapter section. Testing without a shroud occurs often, simply because the shroud is not available or the test facility considerations favor a smaller test-article envelope.

It is often believed that by removing the shroud and imposing acoustic test levels representative of the environment interior to the shroud, a satisfactory test can be performed. However, it has been observed[1] that the response from a shroud-removed acoustic test does not, in general, satisfactorily duplicate the response obtained with the shroud installed. The noted reduction in response level when the shroud is removed indicates a significant loss of vibrational energy that ordinarily would have traveled the mechanical path via the shroud, and thus, the test yields an undersimulation of the structure response of the spacecraft.

Similarly, a random vibration test is often performed in the belief that mechanical excitation can be input at the base of the spacecraft such that all significant regions of the spacecraft will be properly excited. This test simulation approach tends to produce a problem opposite to that encountered when the acoustic test is performed on the spacecraft alone. That is, where the acoustic test may tend to generate satisfactory responses in regions far removed from the spacecraft base but highly unsatisfactory responses near the base, the opposite situation is likely to occur in the base vibration test approach.

In view of this background, a research test program was conducted to evaluate the degree to which various test configurations can adequately simulate an acoustic environment. Recognizing the fact that a test often cannot be performed in the most optimum fashion, the research test program was designed to provide information from two points of view. One viewpoint was that of investigating the magnitude of the test input change necessary to produce the desired output response and the difficulty in producing such a change. The other aspect was that of observing the degree of missimulation that can possibly result from performing a particular less-than-optimum test, which is typical of what is often done.

Based on an evaluation of the test results, spacecraft test guidelines were developed which can be helpful when performing a test simulation of the launch acoustic environment.

TEST DESCRIPTION

Test Item

The structural test model employed in this investigation (figure 1) was designed in-house to satisfy specific requirements in the overall test program. The model was to simulate a typical spacecraft, spacecraft adapter, shroud, and lower support structure, and was to be of appropriate overall physical size to allow testing in the Goddard Space Flight Center 68-m^3 reverberant acoustic test chamber. An additional requirement was that the model be adaptable for convenient modification to produce various configurations (for example, equipment shelves that can be loaded and unloaded, panels of different thickness and construction,

spacecraft and shroud connection interface at different location levels, provision for attachment of booms and paddles, and adapters of different designs).

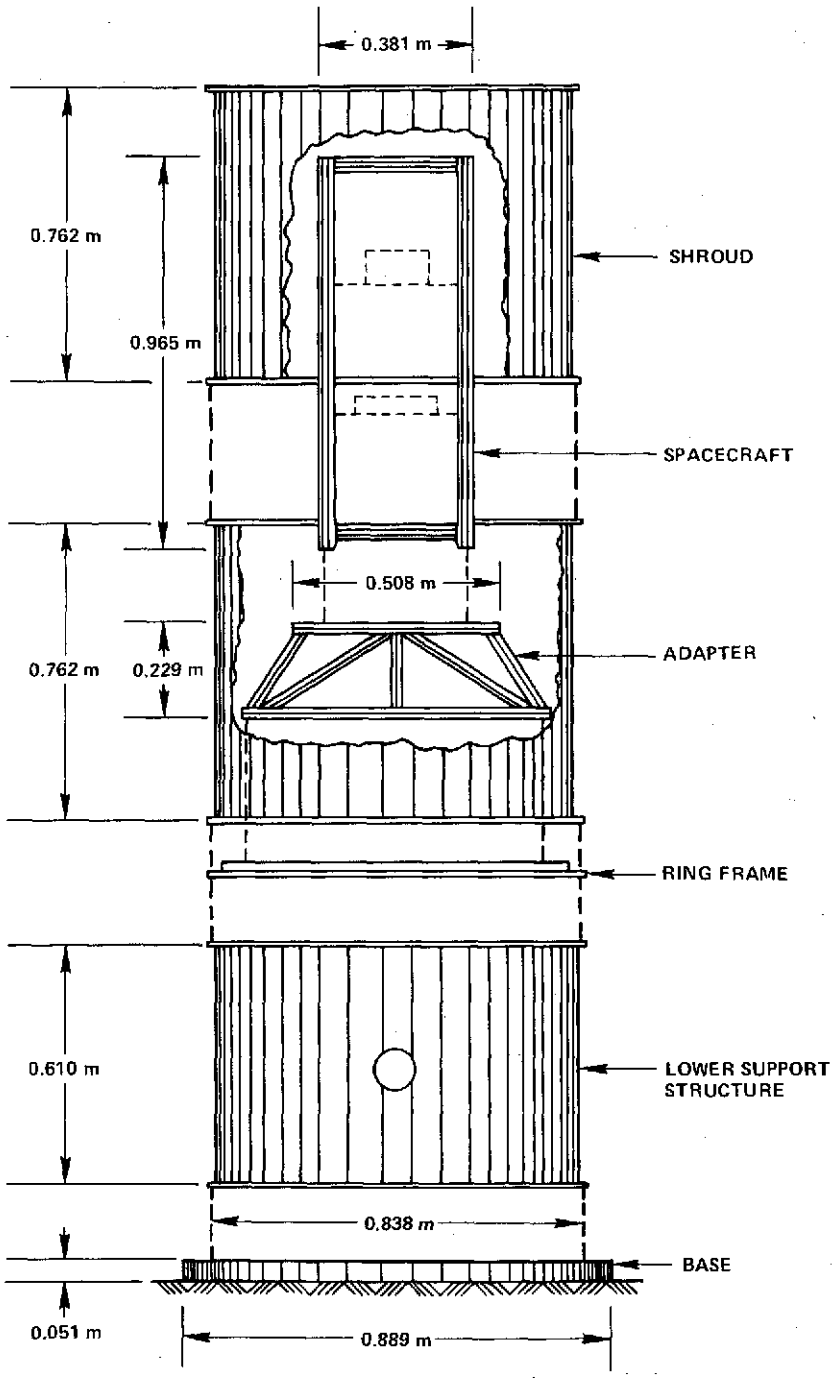

Figure 1. Exploded view, acoustic test model.

Physical Properties of Test Model

Physical properties of the test model components are summarized below.

Spacecraft

L X W X H: 0.38 m X 0.38 m X 0.94 m
Material: Al 6061-T6
Side Panels: 0.00127 m
1.15 kg per panel

Equipment Shelves		Thickness (m)	Equivalent Weight (kg)
Top	1	0.00159	0.55
Center	2	0.00318	2.89
	3	0.00396	3.20
Bottom	4	0.00635	2.18

Adapter

Truss Frame: Constructed of 0.0254 m X 0.0254 m aluminum bars
Total Weight: 7.76 kg

Shroud

Outside Diameter: 0.84 m
Length: 1.5 m
Material: AL 6061-T6 Shell
Wall Thickness: 0.00127 m
Ring Frequency: 1920 Hz
Critical Frequency: 10200 Hz
Baffles: 0.0254 m Plywood
0.00127 m Rubber
0.00635 m Aluminum
Total Weight: 32.9 kg

Lower Support Structure and Ring Frame

Outside Diameter: 0.84 m
Length: 0.61 m
Material: Al 6061-T6 Shell
Wall Thickness: 0.00318 m
Ring Frequency: 1920 Hz
Critical Frequency: 5000 Hz
Ring Frame: Aluminum ring with overall thickness of 0.0508 m
Total Weight: 42.2 kg

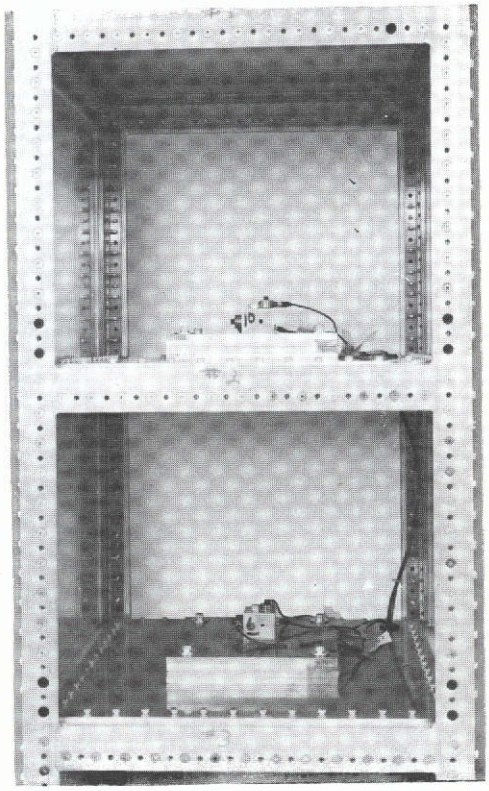

Figure 2. Spacecraft equipment shelves.

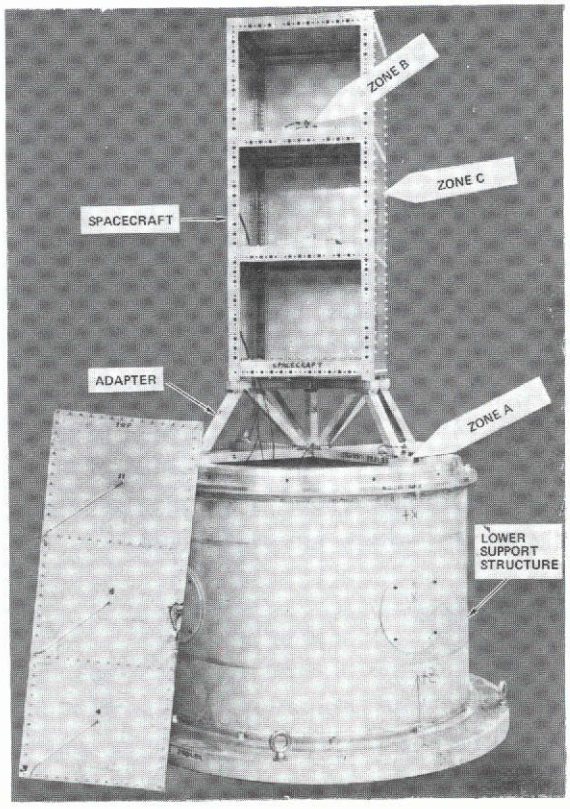

Figure 3. Baseline test model with shroud removed, showing location of test zones.

The structural model representing the spacecraft-adapter truss package had a total weight of about 30 kg with a total length of 1.2 m from the base of the adapter to the top of the spacecraft. The central box structure, measuring 0.38 m by 0.38 m by 0.94 m was formed from thin solid aluminum sheets. The equipment shelves (figure 2) consisted of solid aluminum panels of different thickness for each shelf and were loaded with additional weights at the second and third shelves from the top of the box to simulate equipment masses. The adapter truss shown in figures 1 and 3 was constructed from aluminum bars.

The shroud consisted of two thin-walled aluminum cylindrical shell halves, joined together to form an overall shroud, with the end sealed off by a baffle consisting of a combination of plywood, rubber, and aluminum panels. For convenience, the typical conical shape of the top of the shroud was not simulated. The ring frequency and critical frequency of the shroud were estimated to be 1.92 kHz and 10.2 kHz, respectively.

The lower support structure below the shroud consisted of an aluminum cylindrical shell, which was connected to the shroud and the spacecraft adapter by a solid aluminum ring frame.

Three different configurations of the test article were required in performing the tests. For the acoustic tests, a baseline or full system model (figure 4), consisting of the spacecraft, adapter, shroud, and lower support structure, was used in obtaining the baseline test results. The acoustic tests of the spacecraft and adapter alone, hereafter also called the shroud-removed tests, were performed using the baseline model with the shroud and lower structure removed. (See figure 5.) This same model was used in the random vibration tests. In tests to assess the effect of the lower support structure on the acoustic response of the spacecraft structure, only the shroud was removed (figure 3).

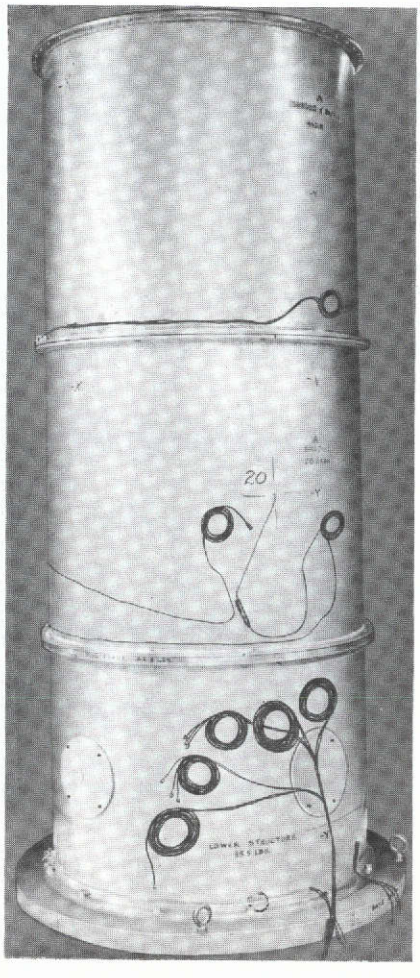

Figure 4. Baseline test model with shroud attached.

Test Facilities

Two test facilities of the Structural Dynamics Branch, Test and Evaluation Division, Goddard Space Flight Center, were used to carry out the research test program. For the acoustic test portion of the investigation, the 68-m^3 reverberant acoustic chamber[2] provided the acoustic noise environment. This facility is capable of producing a reverberant acoustic environment of 160 dB in overall sound pressure level (OASPL) with a continuous spectrum from 31.5 Hz to 10 kHz.

For the random vibration test portion of the study, the C210 electrodynamic shaker was used to generate the mechanical random vibration environment. This facility has a force capability of 1.1×10^5 N (25,000 lb) from 20 Hz to 2 kHz, with a shaping capability in the dynamic range of 30 to 35 dB.

Test Setup

Figure 5 shows the suspension of the spacecraft and adapter for a typical acoustic test in the reverberant noise chamber, and the mechanical setups for a typical random vibration test on the C210 shaker system are shown in figures 6 and 7.

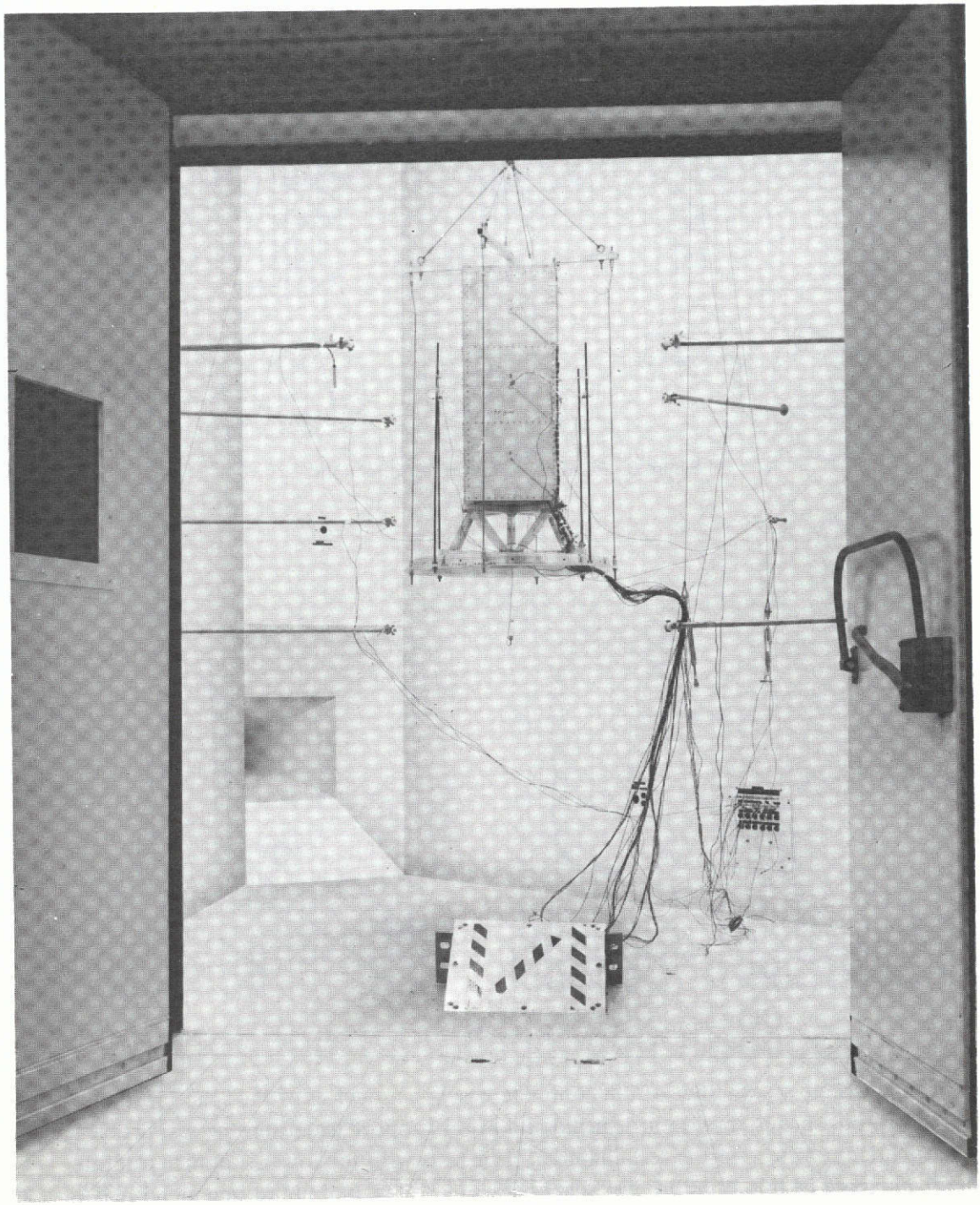

Figure 5. Setup for acoustic test of spacecraft and adapter.

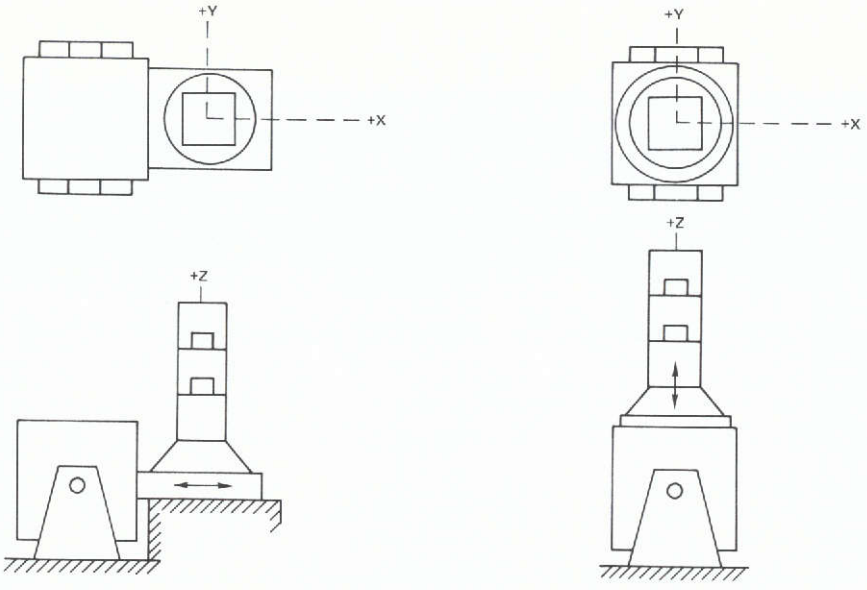

Figure 6. Random vibration test directions.

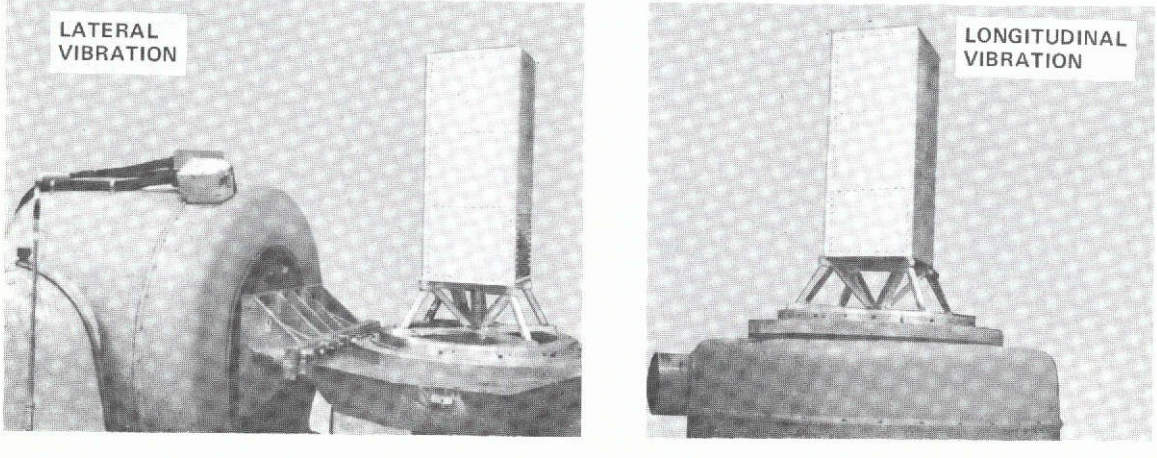

Figure 7. Setups for random vibration tests.

For the acoustic tests, whether of the complete baseline model or of the spacecraft and adapter without shroud or without shroud and lower support structure, the test article was suspended overhead in the test chamber. For tests with the lower support structure present, the base of this structure was suspended at a distance of about one meter above the chamber floor, with the spacecraft longitudinal axis (z-axis) aligned with the center of the room. For all tests, the test items were located at elevations normally occupied as if the full system model were present.

All locations and orientations described in this report were referenced to the spacecraft orthogonal axes as defined in figure 8.

Instrumentation

Forty accelerometers at 24 different locations were used to monitor the model's dynamic response. Table 1 and figures 8, 9, and 10 present a detailed tabulation of the accelerometer designations and a description of their locations. The accelerometer locations were divided into four general groups:

- Accelerometers on the spacecraft adapter (6 total, 2 locations);
- Accelerometers on the spacecraft equipment shelves within the spacecraft box (6 total, 2 locations);
- Accelerometers on the spacecraft box (15 total, 9 locations); and
- Accelerometers on the shroud and lower structure (13 total, 11 locations).

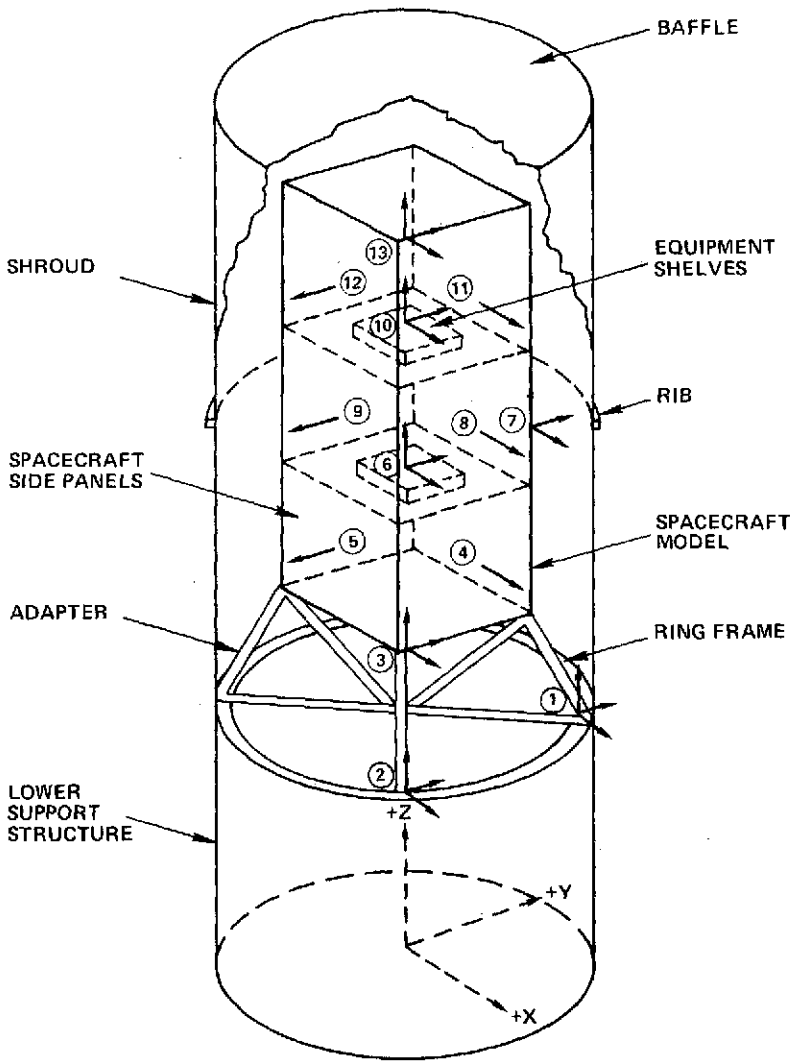

Figure 8. Accelerometer locations on spacecraft and adapter.

The mounting locations listed above were chosen to determine the differences among the responses monitored from primary structural members (group 1), from the basic structure that supports and encloses the spacecraft experiments (group 2), and from the spacecraft box (group 3). Group 4 locations were monitored for the purpose of assessing the dynamic characteristics of the shroud and lower structure.

Table 1
Accelerometer Locations

Location	Accelerometer	Descriptive Location
1	1x, 1y, 1z	Base of spacecraft adapter
2	2x, 2y, 2z	Base of spacecraft adapter
3	3x, 3y, 3z	Corner base of spacecraft box
4	4x	Lower spacecraft side panel
5	5y	Lower spacecraft side panel
6	6x, 6y, 6z	Center of weight on third experiment shelf
7	7x, 7y, 7z	Middle spacecraft side panel corner
8	8x	Middle spacecraft side panel
9	9y	Middle spacecraft side panel
10	10x, 10y, 10z	Center of weight on second experiment shelf
11	11x	Upper spacecraft side panel
12	12y	Upper spacecraft side panel
13	13x, 13y, 13z	Corner of top experiment shelf
14	14n	Upper shroud
15	15n	Middle shroud
16	16n	Middle shroud
17	17n	Lower shroud
18	18n	Lower shroud
19	19n	Lower shroud
20	20n	Lower shroud directly opposite to 18n
21	21n	Top of lower structure
22	22n	Middle of lower structure
23	23x, 23y, 23z	Base of lower structure
24	24n	Middle of lower structure directly opposite to 22n

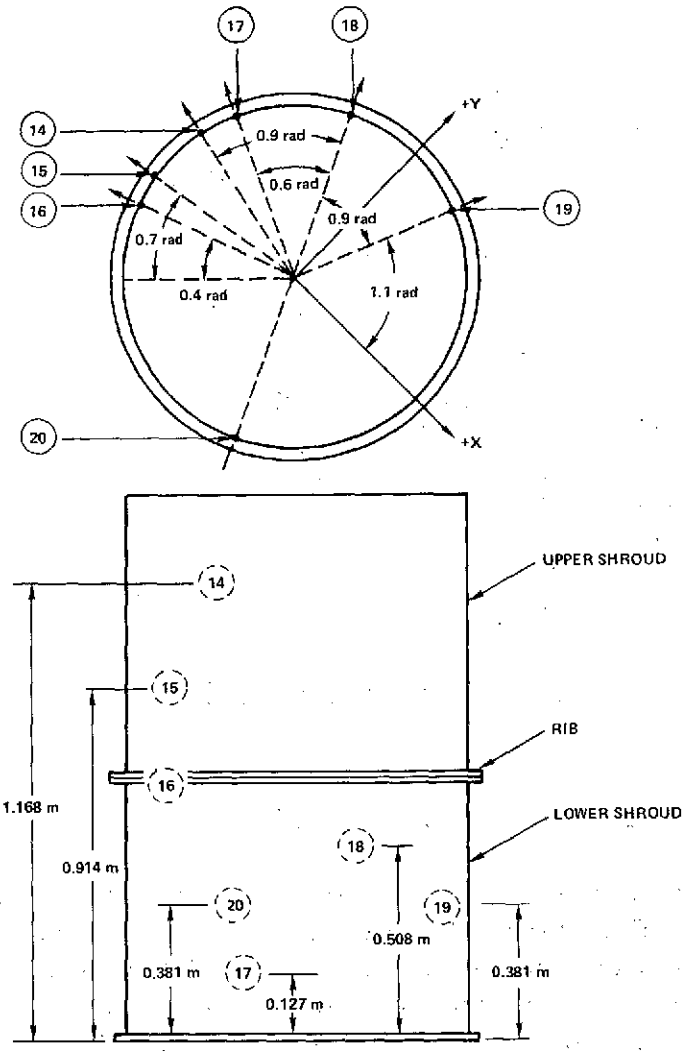

Figure 9. Accelerometer locations on shroud.

Sixteen microphones were installed to monitor the acoustic excitation exterior and interior to the shroud. Table 2 and figure 11 illustrate their mounting locations. Control microphones are numbered 103 to 106 for the shroud-installed acoustic tests and 111 to 114 for the shroud-removed acoustic tests. During each test the microphone and accelerometer responses were recorded on magnetic tape. Selected channels were also displayed on oscillograms to provide quick-look analyses and to ensure nonclipping of data.

TEST PROCEDURES

Figure 12 presents in block diagram form the logic upon which the overall research test program was based. A baseline or full system test model and an arbitrary acoustic environment were assumed to be the realistic service system and environment. The complete

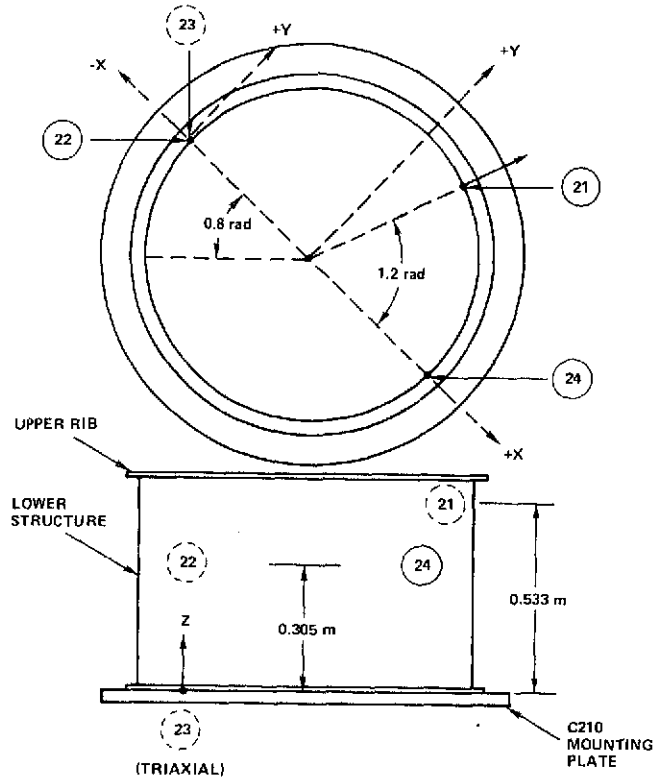

Figure 10. Accelerometer locations on lower support structure.

baseline test model was subjected to the acoustic environment, and the resultant acceleration response at significant structural points was recorded. The average acceleration response at the three zones listed in table 3 represents the test levels to be simulated by reverberant acoustic tests on the spacecraft without the shroud and lower structure and without the shroud only. Lateral and longitudinal acceleration responses were also to be simulated separately by random vibration tests on the spacecraft without the shroud and lower structure. The results of the simulated tests were then extensively compared to the results of the baseline model test on the basis of one-third-octave band acceleration levels and overall response levels.

Figure 13 shows the flow diagram used in performing the acoustic test simulation. This diagram summarizes a transfer function procedure (see Appendix) for shaping the required acoustic input for the spacecraft and adapter model tests. Figure 14 indicates the flow diagram for the random vibration tests.

Acoustic Test Procedures

The first series of tests performed were the acoustic tests. A sound pressure level (SPL) spectrum which typifies a realistic launch acoustic environment was used as the input for the baseline acoustic test. The acceleration response results from the baseline test were

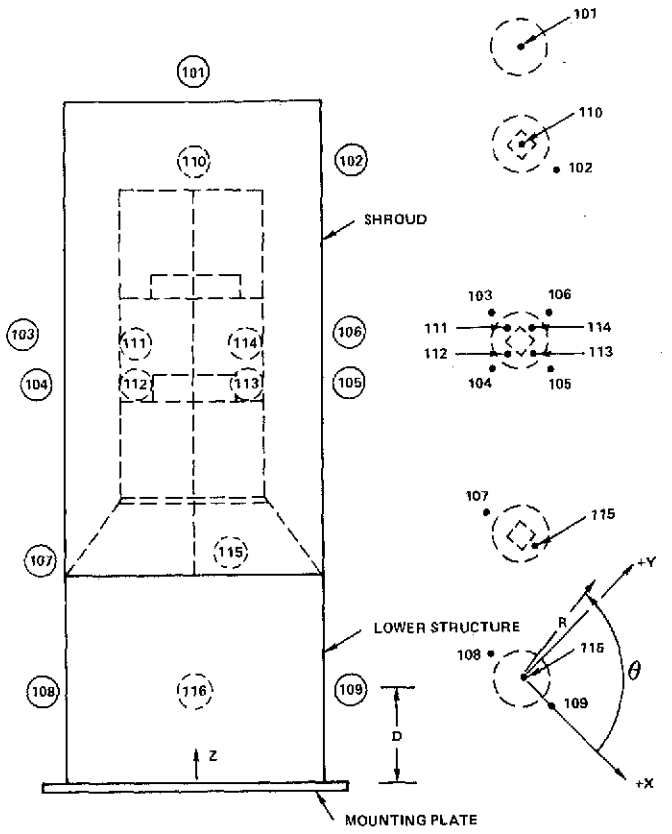

EXTERNAL MIKES, 101 TO 109; CONTROL MIKES, 103, 104, 105, 106.
INTERNAL MIKES, 110 TO 116; CONTROL MIKES, 111, 112, 113, 114.

Figure 11. Microphone locations. (Right, the horizontal dispersion.)

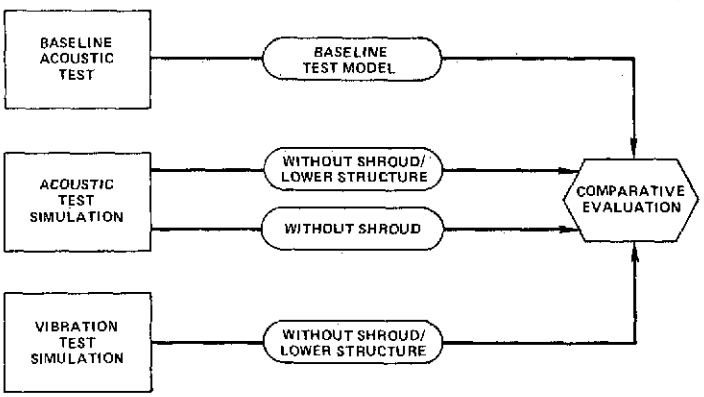

Figure 12. Overall test program logic.

Table 2
Microphone Locations

Microphone Number	Type	Radius from Z-axis (Meters)	Angle θ (Radians)	Distance from Base (Meters)
101E*	B&K	0	–	2.286
102E	B&K	0.838	0	2.007
103E	B&K	0.838	3.14	1.422
104E	B&K	0.838	4.71	1.422
105E	B&K	0.838	0	1.422
106E	B&K	0.838	1.57	1.422
107E	B&K	0.838	3.14	0.787
108E	B&K	0.838	3.14	0.279
109E	B&K	0.838	0	0.279
110 I	B&K	0	–	2.007
111 I	B&K	0.305	3.14	1.422
112 I	B&K	0.305	4.71	1.422
113 I	B&K	0.305	0	1.422
114 I	B&K	0.305	1.57	1.422
115 I	B&K	0.356	0	0.787
116 I	B&K	0	–	0.279

*External to shroud
†Internal to shroud

Table 3
Spacecraft Zones

Acoustic Tests		
Zone	Location	Baseline Response Simulation
A	Base of spacecraft adapter	Space average of 1x, 1z, 2y
B	Spacecraft upper dummy equipment mass	Space average of 10x, 10y, 10z
C	Spacecraft side panels	Space average of 12y, 8x, 9y, 4x
Vibration Tests		
Ax	Base of spacecraft adapter	Space average of 1x, 2x
Bx	Spacecraft upper dummy equipment mass	10x
Cx	Spacecraft side panels	Space average of 4x, 8x, 11x
Az	Base of spacecraft adapter	Space average of 1z, 2z
Bz	Spacecraft upper dummy equipment mass	10z

then used to generate the desired test levels to be simulated by the acoustic and random vibration test on the spacecraft and adapter without the shroud and lower structure.

The effect of the removal of the shroud and lower structure on the spacecraft response was evaluated by subjecting the spacecraft and adapter model to the internal sound pressure level, and then comparing the response results with the baseline test responses. The influence of the lower structure was investigated by repeating the acoustic tests with the lower structure in place and comparing the responses with the responses obtained without the lower structure. Described below is the sequence of tasks performed for the acoustic tests.

Task 1, Baseline Acoustic Test (See figure 13)

Using the complete baseline test model, an acoustic noise test was accomplished. This test provided the baseline data, indicating the acoustic response of the spacecraft with adapter, shroud, and lower support structure. All subsequent tests without the shroud were designed to simulate the baseline response results.

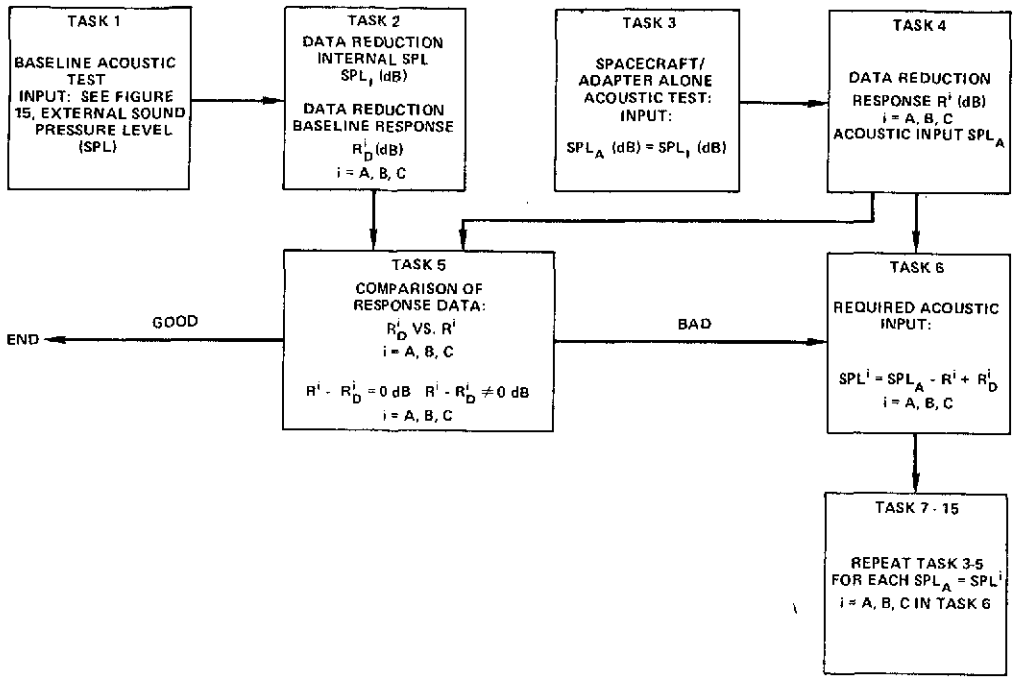

Figure 13. Flow diagram for acoustic tests.

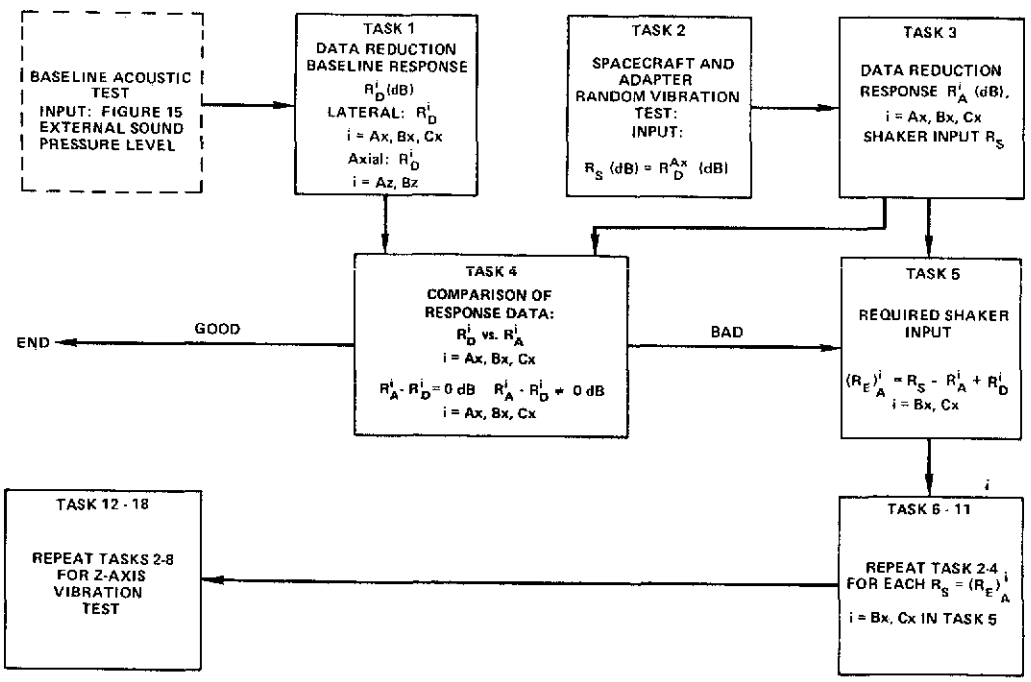

Figure 14. Flow diagram for random vibration tests (controlling at location Ax)

The acoustic excitation was controlled to match the external SPL shape of figure 15, at an OASPL of 141 dB for a test duration of 30 seconds. Outputs from micrphones external and internal to the shroud and lower structure, and from accelerometers on the spacecraft, adapter, shroud, and lower structure were recorded on magnetic tape. Quick-look analysis, using an oscillograph recording, was performed during this test, and during all subsequent tests, to assure nonclipping and adequate gain settings during data acquisition.

Task 2, Data Reduction

The second task was to obtain acceleration response (R_D^i) and internal acoustic level (SPL_I) from the baseline acoustic test. Using the data tape from task 1, R_D^i and SPL_I data were generated for use in the acoustic test (task 3) of the spacecraft and adapter model. Space-averaged, one-third octave band level (OBL) and overall level (OAL) response data were determined for each of the three spacecraft zones which are listed in table 3. The results for each zone are designated by the superscript i in R_D^i as A, B, and C for convenience.

Task 3, Spacecraft and Adapter Acoustic Test

Using the test model with shroud and lower structure removed, an acoustic noise test was performed. The acoustic input was controlled to match the SPL_I results from task 2 (baseline internal SPL), for 30 seconds duration, through the use of control microphones 111 to 114. Each zone was considered as a separate simulation effort. For example, the first test of task 3 was an attempt to simulate the averaged one-third OBL response of acceleration channels 1x, 1z, and 2y, that is, zone A.

Task 4, Data Reduction

The task here was to obtain acceleration response R^i and acoustic input SPL_A from the spacecraft/adapter acoustic test. Using data tape from task 3, R^i and SPL_A data were generated, in a manner similar to task 2, for use in comparison with baseline response (task 5), and in modifying, if required, the acoustic input (task 6) for subsequent tests of the spacecraft and adapter model.

Task 5, Comparison of Response Data

The results of the data reduction, task 4 (R^i), were compared on a one-third OBL and OAL basis with R_D^i from task 2.

Task 6, Computation of Required Acoustic Input

Using appropriate data from task 4 and task 2, as shown in the flow diagram, figure 13, the required acoustic excitation SPL^i for use in acoustic simulation tests, was determined to simulate the acceleration response in each zone (i = A, B, C).

Task 7 through Task 15

These tasks consisted of repeating tasks 3 through 5 for each SPL^i (i = A, B, C) as determined by task 6 to verify the magnitude of the test input change which would be necessary to produce the desired output response, and to access the difficulty in producing such a change due to facility limitations.

Random Vibration Test Procedures

The final series of tests performed were the random vibration tests. The primary objective of these tests was to generate spacecraft and adapter alone responses, using mechanical excitation, which would be comparable to the baseline responses. The flow diagram for the random vibration tests was shown in figure 14.

Since multidirection and multipoint shaking were beyond the capability of the C210 vibration test facility, only single-axis vibration tests were conducted. The vibration responses in the x- and z-directions (figure 7), as specified in table 3, were determined. Two methods of control were used. First, control of the vibration input in each axis was based on the average of single-axis responses at locations on the control interface, defined as the base of the spacecraft adapter. Second, vibration tests were also performed by servocontrolling directly off the accelerometers mounted in each zone for which the response was being simulated. The results provided an assessment of these two methods of vibration control.

The logic applied in the random vibration tests was similar to that employed for the acoustic simulation tests. In this case the acoustic excitation was replaced by a single axis random vibration input from a shaker. Transfer functions between the control and response points of interest were determined from data obtained in an initial random vibration test (task 2). These transfer functions were then applied to shape the shaker input to the levels required to produce the desired acceleration response.

Presented below is a summary of the task sequence used for the vibration tests.

Task 1, Data Reduction (See figure 14)

The task here was to obtain acceleration response (R_D^i) from the baseline acoustic test. Using data from acoustic task 1, R_D^i (i = Ax, Bx, Cx, Az, Bz) data were generated for the x-axis and z-axis vibration tests of the spacecraft and adapter model (table 3).

Task 2, Spacecraft and Adapter Random Vibration Test

The initial task in the x-axis random vibration simulation was to perform a single-axis random vibration test in the x-direction, as shown in figures 7 and 8. The vibration input for this test, R_S, was controlled to match R_D^{Ax} of task 1 for zone Ax (table 3, Vibration Tests) over a test period of 30 seconds.

Task 3, Data Reduction

Here the task was to obtain the acceleration response (R^i_A) from the spacecraft and adapter vibration test. Using data from task 2, R^i_A data (i = Ax, Bx, Cx) was generated for comparison with the baseline response (task 1) information.

Task 4, Comparison of Response Data

The results of the task 3 data reduction of the x-axis vibration (R^i_A) were compared with the task 1 baseline acoustic test result (R^i_D) on a one-third OBL and OAL basis.

Task 5, Required Shaker Input

Using appropriate data from tasks 3 and 1, as shown in figure 14, the required input $(R_E)^i_A$ for each x-axis, the random vibration simulation (i = Bx, Cx) for input at the adapter base was determined.

Tasks 6 through 11

These tasks consisted of repeating tasks 2 through 4 for each $(R_E)^i_A$ (i = Bx, Cx), as determined by task 5, to verify the magnitude of the test input change which would be necessary to produce the desired output response and the difficulty in producing such a change. Note that because simulation of Ax was performed essentially by task 2, only the two additional cases (Bx and Cx) remained to be simulated.

Task 12 through Task 18

For these tasks, tasks 2 through 8 were repeated for the z-axis vibration test.

DATA REDUCTION AND ANALYSIS

Data reduction and analysis for the investigation required both quick-look and off-line data reduction capabilities. The quick-look data requirement was an in-line event; that is, information from each run was required prior to continuing the test, and rapid response was mandatory in producing the required data as specified under Test Procedures, above. Off-line data reduction was used for post-test detailed analysis of the test data which was recorded on tape.

In the analysis of accelerometer and microphone data, one-third octave band levels of acceleration and sound pressure and overall levels were obtained, using a General Radio one-third octave band analyzer, model 1921. This analyzer has accuracy limits estimated to be ±1 dB. The overall system accuracy limits, inclusive of errors in calibrations and shaping of sound pressure levels or acceleration levels, was estimated to be ±2 dB.

RESULTS

Baseline Acoustic Test

The results of the baseline acoustic test are presented in the graphs, figures 15 through 21.* In figure 15 the external SPL used to excite the baseline test model is shown as the solid curve. The corresponding measured internal-to-shroud SPL is depicted by the dashed curve. The noise reduction ($SPL_{Ext.} - SPL_{Int.}$) obtained for the shroud is shown in figure 16.

The averaged acceleration responses to the external SPL of figure 15 at the base of the spacecraft adapter (zone A), at the spacecraft upper dummy equipment mass (zone B), and at the spacecraft side panels (zone C), relative to the external and internal SPL, are presented in figures 17 through 19.

The selected lateral and axial baseline test responses at zones A, B, and C, for which response simulation was investigated through the use of vibration tests, are shown in figures 20 and 21.

Acoustic Tests of Spacecraft and Adapter

The results of the acoustic tests conducted on the spacecraft and adapter, without the shroud and lower structure, are presented in figures 22 through 33 and table 4. Figures 22 through 24 show the average acceleration response for zones A, B, and C (relative to the baseline test response) which results from the baseline internal SPL as input.

The acceleration response to acoustic SPL input transfer functions, used for the acoustic test simulation of responses at zones A, B, and C, are shown in figures 25 through 27.

Modifications to the acoustic inputs theoretically required to simulate zone A, B, and C baseline acceleration responses are presented in figures 28 through 30, respectively, by the open-circle curve. The actual inputs that were attainable during the test are shown by the black-circle curve.

Figures 31 through 33 and table 4 present the results of the acoustic test simulations for the spacecraft and adapter only, without the shroud and lower structure. These results are plotted relative to the baseline test results for comparison. Plot (a) of the figures presents the comparison of the simulated zone A, B, or C responses. Plots (b) and (c) correspond to the comparison of resultant responses at the other two zones. Table 4 summarizes a comparison of simulated, overall-level zonal responses. Because of the inability of the test facility to produce the desired acoustic input band levels of figure 28, the results in figure 31 have been adjusted by adding (or subtracting) the band level difference between the desired input and the actual input.

*For convenience, the graphs, figures 15 through 63, are placed at the end of the text.

Table 4
Comparison of Overall Zonal Response, Acoustic Tests,
Spacecraft and Adapter Only

(Results from Figures 31 to 33)

Zonal Response Simulated	Resultant OAL Response Relative to Baseline Results		
	Zone A	Zone B	Zone C
Zone A (See Figure 31)*	+1 dB	+9 dB	+11 dB
Zone B (See Figure 32)	-8 dB	+2 dB	+ 2 dB
Zone C (See Figure 33)	-7 dB	-1 dB	0 dB

*Results compensated for test facility limitations.

Spacecraft, Adapter, and Lower Support Structure Acoustic Tests

The results of the acoustic tests conducted on the spacecraft model without the shroud are presented in figures 34 through 45 and table 5. The average zone A, B, and C acceleration responses (relative to the baseline test response), generated with the baseline internal SPL as input, are shown in figures 34 through 36.

Figures 37 through 45 and table 5 present the results of the investigation to improve the simulation of the zonal responses by including the lower structure in the acoustic tests.

The transfer functions shown in figures 37 through 39 were used during the acoustic test to generate the required acoustic inputs shown as solid lines on figures 40 through 42. The inputs actually achieved are shown as dashed lines.

In figures 43 through 45 and table 5, the acoustic test simulation results are presented and evaluated similar to previous test simulation results. The results have been compensated for the test facility limitations.

Lateral Vibration Tests (X-axis)

The results from the simulation of the baseline lateral responses, shown in figure 20, by random vibration tests are presented in figures 46 through 57 and table 6. In figure 46, the ability to simulate the desired zone Ax lateral acceleration levels, using a vibration

Table 5
Comparison of Overall Zonal Response, Acoustic Tests,
Spacecraft, Adapter, and Lower Support Structure

(Results from Figures 43 to 45)

Zonal Response Simulated	Resultant OAL Response Relative to Baseline Results		
	Zone A	Zone B	Zone C
Zone A (See Figure 43)*	+ 1 dB	+11 dB	+13 dB
Zone B (See Figure 44)*	-10 dB	+ 2 dB	+ 4 dB
Zone C (See Figure 45)*	- 5 dB	+ 1 dB	+ 2 dB

*Results compensated for test facility limitations.

Table 6
Comparison of Overall Lateral Response, Lateral Vibration Tests,
Spacecraft and Adapter Only

(Results from Figures 46-48, 51-53, 56-57)

Zonal Response Simulated	Resultant OAL Response Relative to Baseline Results					
	Zone Ax		Zone Bx		Zone Cx	
	Servo-control	Transfer Function	Servo-control	Transfer Function	Servo-control	Transfer Function
Zone Ax (See Figures 46, 47)*	0 dB	N.A.†	- 2 dB	N.A.†	-24 dB	N.A.†
Zone Bx (See Figures 48, 51, 52)*	+ 8 dB	+ 5 dB	0 dB	- 1 dB	-20 dB	-20 dB
Zone Cx (See Figures 53, 56, 57)*	+35 dB	+25 dB	+27 dB	+26 dB	0 dB	+ 1 dB

*Results compensated for test equipment limitations.
†Not applicable.

equalizer system, is demonstrated. The simulation result actually obtained during the test is indicated by plot (a). Plot (b) of figure 46 shows the result which was obtained when the test equipment limitations were totally compensated for.

The resultant zone Bx and Cx lateral responses generated by the zone Ax simulation are shown in figure 47. These results have also been adjusted to normalize out the effect of vibration system limitations.

Figures 48 through 52 indicate the results of the lateral vibration simulation of the zone Bx baseline response.

Figure 48 demonstrates the closeness to which perfect simulation of the zone Bx baseline response can be obtained by two methods. The first method is servocontrol directly on the zone Bx response. Plot (a) presents the simulation result actually obtained by this method. Secondly, figure 48 shows the method of servocontrol at zone A at the base of the adapter. The result of this method is shown in plot (b), which demonstrates the simulation that is obtained by the transfer function approach when the results are compensated for the test equipment limitations. Plot (c) is a modification of plot (a) which results when plot (a) is compensated for the test equipment limitations.

Figure 49 shows the transfer function which was used to develop the required input shown in figure 50.

Figures 51 and 52 present the responses at zones Ax and Cx which result from the simulation of zone Bx by each of the two methods of control. These results also have been adjusted to compensate for the equipment limitations. Figures 53-57 show the similar results from the lateral vibration simulation of the zone Cx baseline response.

Longitudinal Vibration Tests (Z-axis)

The results which demonstrate the ability to simulate the zone Az and Bz longitudinal baseline responses (figure 21) by the longitudinal vibration test are presented in figures 58 through 63 and table 7. Figure 58 shows the ability to simulate the zone Az acceleration response by use of a vibration equalizer system. Figure 59 shows the resultant zone Bz response generated by the zone Az simulation. Note that the results of plot (b) of figure 58 and figure 59 have been compensated for the equipment limitations.

The ability to simulate the zone Bz response by use of direct servocontrol and by the transfer function method is demonstrated by the results shown in figure 60. The resultant zone Az response generated by the simulation of zone Bz response is presented in figure 61. Figures 62 and 63, respectively, show the transfer function and shaker input used in the zone Bz response simulation.

Table 7
Comparison of Overall Axial Response, Axial Vibration Tests,
Spacecraft and Adapter Only

(Results from Figures 58-61)

Zonal Response Simulated	Resultant OAL Response Relative to Baseline Results			
	Zone Az		Zone Bz	
	Servo-control	Transfer Function	Servo-control	Transfer Function
Zone Az (See Figures 58, 59)*	+ 1 dB	N.A.†	-1 dB	N.A.†
Zone Bz (See Figures 60, 61)*	+12 dB	-6 dB	-1 dB	-2 dB

*Results compensated for test equipment limitations.
†Not applicable.

DISCUSSION OF RESULTS

The results of the acoustic test portion of this investigation (figures 22 through 45 and tables 4 and 5) demonstrate the need and the ability to simulate the total shroud effects in acoustic tests of spacecraft structures with the shroud removed. In a comparative evaluation of the total results, several factors were considered:

- Overall level deviations greater than ±2 dB (from 0 dB) were considered significant variations from the baseline overall level.
- Relative acceleration band level spectra deviations outside of a best fit 4-dB amplitude band were considered significant variations from baseline results.
- Evaluation of results were limited to frequencies greater than 100 Hz, due to test chamber performance degradation below this frequency.
- In evaluating results from test simulations, consideration was given to the degree of attainment in shaping the spectra to the desired spectra during the actual test. This was prompted by inabilities to attain the desired test levels, because of limitations inherent in the acoustic and vibration excitation systems. In the acoustic tests the problem was attributed to limitations associated with the acoustic driver-horn-equalizer system, and in the vibration tests the problem was related primarily to the inability to shape the desired input spectrum using the system equalizer. Accordingly, to normalize out the effect of this problem on the evaluation of the results of the study, test response results were scaled when necessary to compensate for the limitations of the test facility.

The test results presented in figures 22 to 24, showing the responses generated at zones A, B, and C without shroud and lower structure, using as input the baseline internal SPL, and in figures 34 to 36, showing the responses for the same zones but without the shroud only, support the earlier belief that acceleration responses from acoustic tests of spacecraft structures with the shroud removed do not, in general, duplicate the responses from the shroud-installed tests.

These results show that when using the internal-to-shroud SPL as inputs, the acoustic tests conducted without the shroud resulted in undertests of 5 to 15 dB. Also, there was a lack of duplication of the response-band-level spectra, predominantly at frequencies of 100 to 500 Hz, in the neighborhood of the low-order shroud modes, where coupling between these modes and the spacecraft adapter is significant.

At substantially higher frequencies, the adapter tends to act as a decoupling element between the spacecraft and the shroud mounting-points, so that direct acoustic excitation of the spacecraft system yielded a closer simulation of the shroud-installed test response. Below the decoupling frequency (<800 Hz), portions of the spacecraft system, for example, zones B and C, responded more significantly to structurally-transmitted vibration from the acoustically-driven shroud than from direct acoustic excitation of the spacecraft without the shroud. This was particularly noticeable for the spacecraft portions located nearest to the shroud attachment ring.

At frequencies above the decoupling frequency (>800 Hz), the spacecraft system tends to respond effectively to the direct acoustic excitation of the spacecraft. This was particularly significant at regions of the spacecraft system which were highly responsive to acoustic excitation and located at some distance from the shroud attachment points, such as the lightweight skin panels of zone C. Undertesting in this frequency range can be alleviated by increasing the acoustic input at frequencies above 800 Hz.

Use of the lower support structure, with space average response similar to the shroud, reduced the undertest at zone A. Due to the absence of the shroud some degradation in band level spectra distribution at low frequencies (<250 Hz) was still noted. This observation was not too surprising, because for frequencies higher than 250 Hz the baseline internal SPL was similar in band level spectra to the baseline external SPL (figure 15). Also, the zone A transfer function—measured with the lower support structure—agreed closer with the baseline than with the transfer function measured without the lower support structure. (See figures 17, 25, and 37.)

The additional energy contributed to the zone A response via the mechanical path of the lower structure was similar in spectra, except below 250 Hz, to that which would be generated if the shroud were installed. At zones B and C no significant improvement in response was noted, because these zones responded more efficiently to direct acoustic excitation, and the contribution from the use of the lower support structure was negligible.

The results of the investigation to improve the simulation of the spacecraft response in shroud-removed tests, by shaping the SPL through the use of a measured transfer function (figures 31 through 33, 43 through 45, and tables 4 and 5), demonstrated that the SPL spectra-shaping methods were more effective for local zone response simulation than for overall spacecraft response simulation.

For example, in figures 31 and 43, the simulation of zone A response did not result in adequate simulation at zones B and C. In this case, an overtest of about 10 dB in OAL occurred for the zone B and C responses. In figures 32 and 44 the simulation of zone B response resulted in an undertest of 9 dB at zone A. Similarly, figures 33 and 45 show that the simulation of zone C response resulted in an undertest of 6 dB at zone A.

The foregoing observations, which were made from the results employing SPL adjustment procedures, were not too surprising, because energy transmission in acoustic response of spacecraft structures is via multiple paths, mechanical and direct acoustical, from input to output. The effectiveness of the SPL-shaping in improving the response at various zones on the spacecraft depends primarily on the relative responsiveness of the zone to energy transmitted by the various forms of transmission. Accordingly, a zone on a spacecraft highly responsive to direct acoustics will respond more effectively to SPL shaping than a zone less responsive to direct acoustics. Conversely, a zone less responsive to direct acoustics but highly responsive to energy transmitted via the mechanical path will respond less effectively to SPL-shaping.

The comparison of results in figures 31 through 33 and figures 43 through 45 indicates that limited improvements in response simulations were obtained from the use of the lower support structure during the acoustic test using SPL spectra adjustments. At frequencies above 400 Hz there was a general improvement in response spectra distribution for the zone A simulation, but insignificant improvement was noted for the resultant zone B and C responses.

In the simulation of zone B response, no significant improvement was noted at zone B, although the zone A and C responses resulting from this simulation showed significant improvement in spectra distribution. In the zone C simulation, a general degradation actually occurred for the zone C response. In this case a significant improvement in spectra distribution was noted for the resultant zone A response, but there was a general degradation for the resultant zone B response.

At frequencies below 400 Hz no significant improvements were noted for all cases of simulated and resultant responses. The absence of the shroud was most evident in the zone A response.

The lack of improvement in simulation when the lower support structure was included in the test is associated with the multipath problem. Inclusion of the lower support structure resulted in two additional paths of transmission, the mechanical and the acoustic paths via the lower support structure, in combination with the original acoustic path. When the

spacecraft is subjected to an SPL (modified on the basis of an acoustical transfer function between a specific spacecraft zone and the acoustic input) which is significantly different spectrally from the baseline input, the response at acoustically responsive zones other than the zone related to the transfer function may be significantly distorted from that desired. For zones (including the zone related to the transfer function) which are less responsive acoustically, limited improvements would be expected from SPL adjustments. The use of the lower support structure was beneficial in all zonal response simulations only when the baseline internal SPL spectra was used as the acoustic input. Accordingly, the use of a lower support structure should be carefully assessed.

The results of the investigation on the use of single-axis random vibration tests on the spacecraft model, without the shroud and lower structure, as a means of simulating the spacecraft baseline lateral and longitudinal responses, are presented in figures 46 through 63 and tables 6 and 7.

The results demonstrated that the simulation of these responses was, in general, limited to the upper frequency cutoff (2 kHz) of the shaker equalizer system, limited to the direction of response corresponding to the shake direction, and was effective only locally. For example, in figures 53 through 57 and table 6, the introduction of the necessary amount of energy at zone Ax to simulate the response at zone Cx of the spacecraft system, located some distance from the shaker input points, resulted in oversimulation of response at zones Ax and Bx.

In figures 46 and 47, simulation of regions on the spacecraft system located nearer the shaker input, that is, zone Ax, resulted in undersimulation at regions farther from the shaker input, at zone Cx. The results of figures 48 through 52 demonstrate the case of simulation of zone Bx which responded about equally to acoustic and mechanical excitation. The result of this simulation was that an overtest and undertest occurred for zone Ax and Cx responses, respectively.

The observations listed above were also noted with regard to the results of figures 58 through 63 for the case of baseline longitudinal response simulation of the spacecraft system. In figure 61, the discrepancy between the zone Az response generated by the two methods of control in the zone Bz simulation could not be explained.

CONCLUSIONS

The ability in some cases of acoustic and random vibration tests of a spacecraft and adapter alone to generate responses which are comparable to the responses produced by a realistic service configuration (consisting of spacecraft, adapter, shroud, and lower support structure) has been demonstrated by the results of this study. Comparative evaluation of these results yields the following conclusions:

- Acoustic tests without the shroud, but with the spacecraft subjected to the interior acoustic levels, cannot in general simulate the true flight responses that result with

the shroud present. Undertesting on the order of 10 dB in acceleration response levels can be expected.

- The test simulation method based on adjusting the acoustic input band levels to account for the absence of the shroud offers an effective approach to the simulation of zonal responses, particularly at regions of the spacecraft removed from the shroud attachment points and for structure that responds efficiently to direct acoustic excitation. The application of this method to overall spacecraft response simulation is limited, in as much as the simulation of one zone may not guarantee adequate simulation at other zones of interest. A simulation achieved for one zone may result in lack of response simulation at another zone by as much as 15 dB.

- The indiscriminate use of a lower support structure during acoustic testing, using the method of adjusting the acoustic input levels, may lead to a simulation actually inferior to a test conducted without the structure. The inclusion of a lower support structure (with average responses similar to those of the shroud) during a test is recommended only in those cases where the internal acoustics are similar spectrally to the external acoustics. Accordingly, the use of a lower support structure should be carefully assessed.

- The use of single-axis vibration tests as a means of simulating the lateral and longitudinal responses is of limited value in the upper frequency range, and is effective only for local regions of the spacecraft in the proximity of the shaker input points which respond efficiently to mechanical excitation. Achieving lateral response simulation at such a region may result in an undertest of greater than 20 dB at regions farther from the shaker input points, regions which are more responsive to direct acoustic excitation.

While the above conclusions relate most directly to the acoustic response simulation problems associated with the spacecraft structural configuration investigated in this study, they are nevertheless considered pertinent as an aid to the development of general approaches for the testing of spacecraft. Based on these conclusions, the following guidelines should be considered when contemplating acoustic response simulation tests on shroud-enclosed spacecraft systems:

- The shroud or a standard shroud fixture, if possible, should be used to provide for the effect of the shroud on the vibroacoustic response of the spacecraft during an acoustic test. This is particularly desirable at frequencies where coupling of lower-order shroud modes with the load-carrying spacecraft support structure is significant. Mechanical excitation of primary load-carrying structural portions may be provided through mechanical vibration testing without the shroud, if it is appropriately performed to cover the lower-frequency range where vibratory stresses in such structures may be significant.

- For secondary structural portions of a spacecraft, well removed from the spacecraft base, such as lightweight skin panel structures, direct acoustic excitation (using SPL shaping) of the spacecraft components should suffice.
- For the overall spacecraft system, when the use of the shroud is prohibited, testing should include direct acoustic excitation of the spacecraft accompanied simultaneously, or sequentially if necessary and appropriate, by mechanical vibration at the spacecraft base. If any a priori knowledge of desired response is available, this information should be utilized to adjust the acoustic excitation input and the mechanical excitation input acceleration level in each frequency band. This will give added assurance that both forms of excitation are adequately covered.

The investigation described in this report was conducted on one particular type of spacecraft structural assembly. The results of this study unfortunately cannot be taken as absolute in providing guidelines for the use in establishing a test approach for all types of structural assemblies. It is suggested that additional studies be made relating to the vibroacoustic response characteristics of other spacecraft structural configurations.

Based on the results obtained from this study, general research areas suggested for further studies include the following:

- Effects of structural parameter variations, such as inclusion of solar arrays: The present study employed a specific test model configuration without solar arrays. Future studies might evaluate the effects on the vibroacoustic energy flow to a spacecraft system, which effects are due to significant changes in the spacecraft structural parameters.
- Transmission path studies: Knowledge of the relative importance of the acoustic path and the mechanical path in acoustic response of shroud-enclosed spacecraft is of considerable value in establishing simulation methods. A significant study might consist of isolating each path successively, to assess its relative contribution to the total spacecraft response for various structural parameters and configurations.

Goddard Space Flight Center
National Aeronautics and Space Administration
Greenbelt, Maryland August, 1974.
502-22-11-01-51

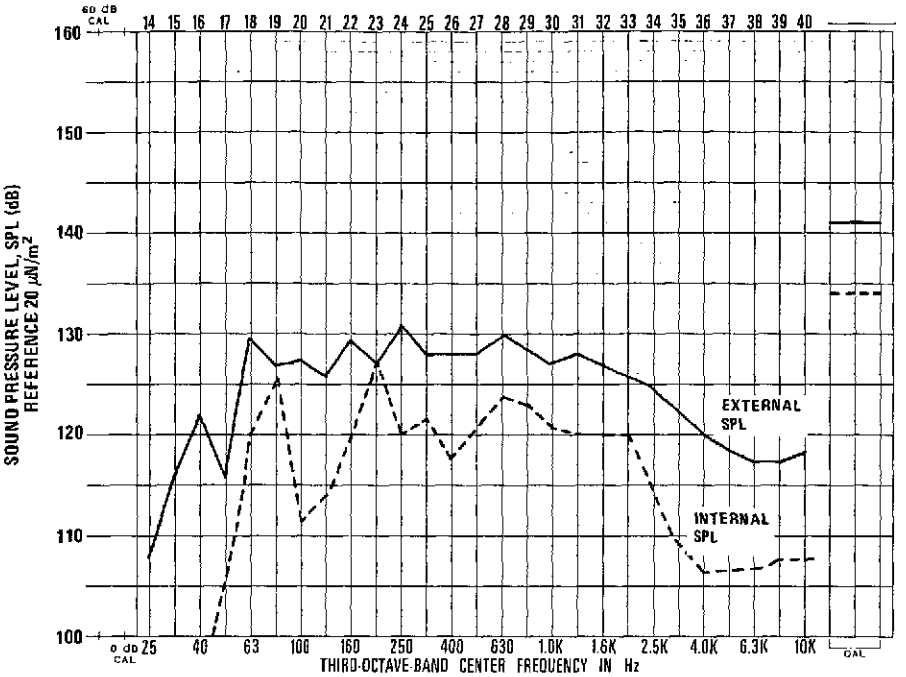

Figure 15. Sound pressure levels of baseline model test.

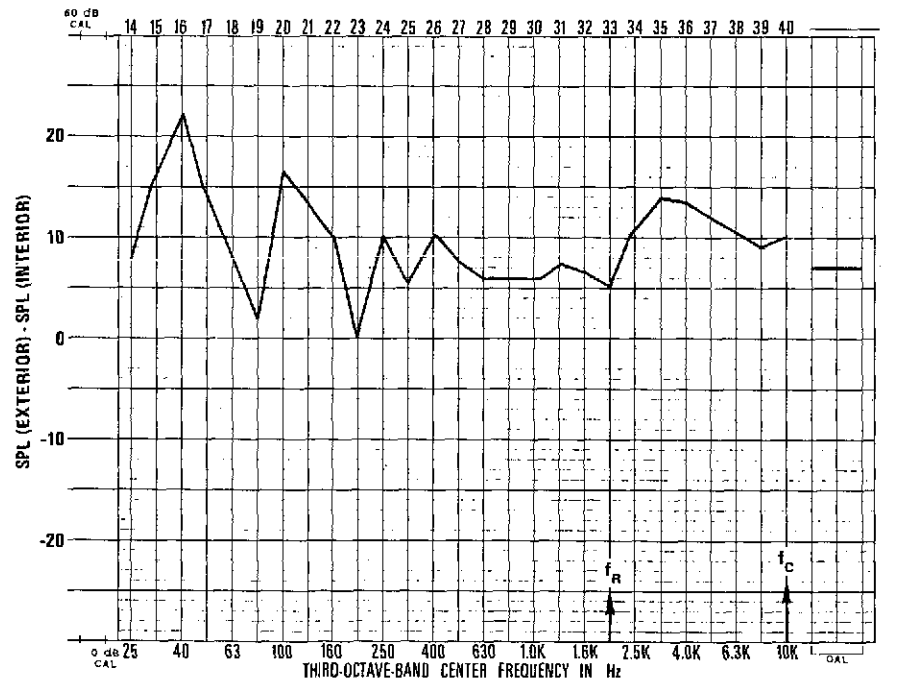

Figure 16. Shroud noise reduction.

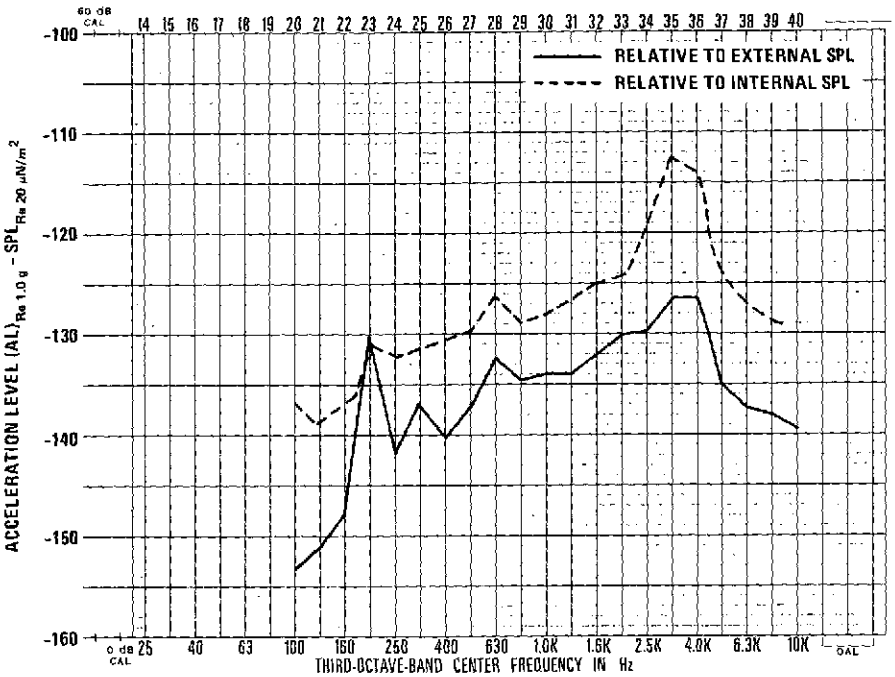

Figure 17. Baseline model acceleration response at zone A, base of spacecraft adapter.

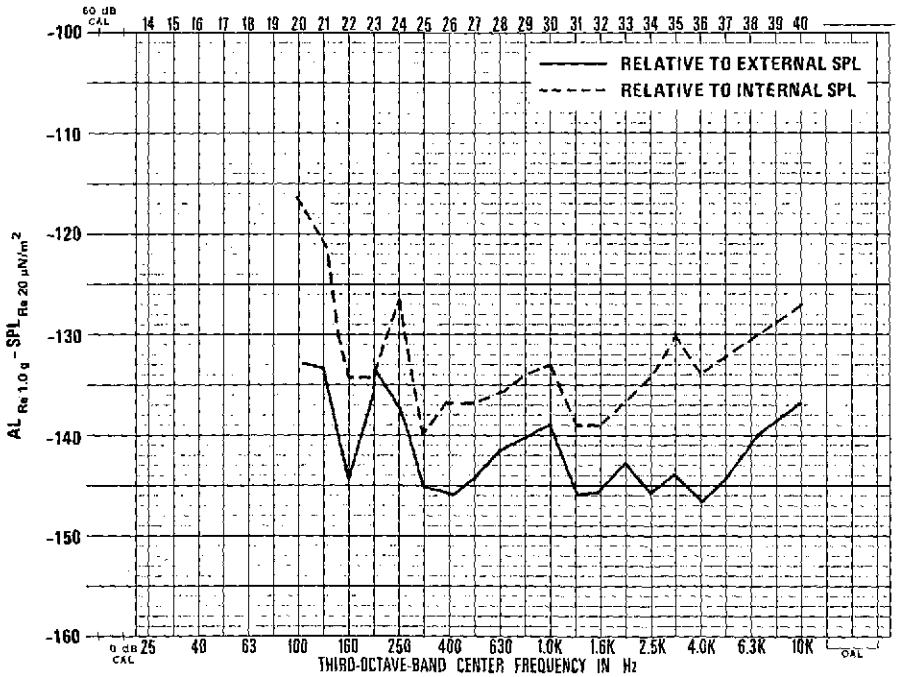

Figure 18. Baseline model acceleration response at zone B, spacecraft upper dummy equipment mass.

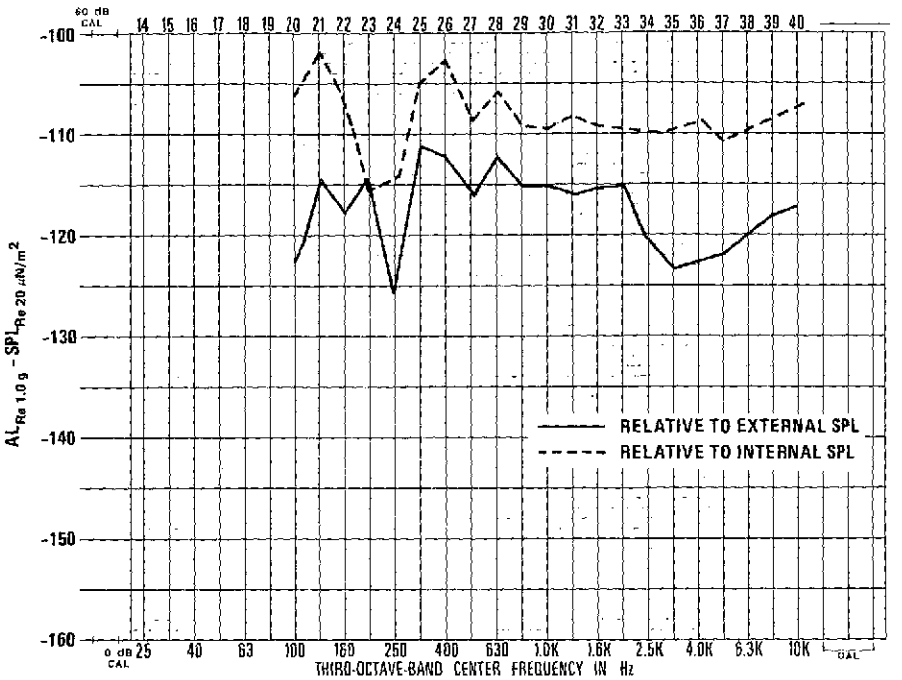

Figure 19. Baseline model acceleration response at zone C, spacecraft side panels.

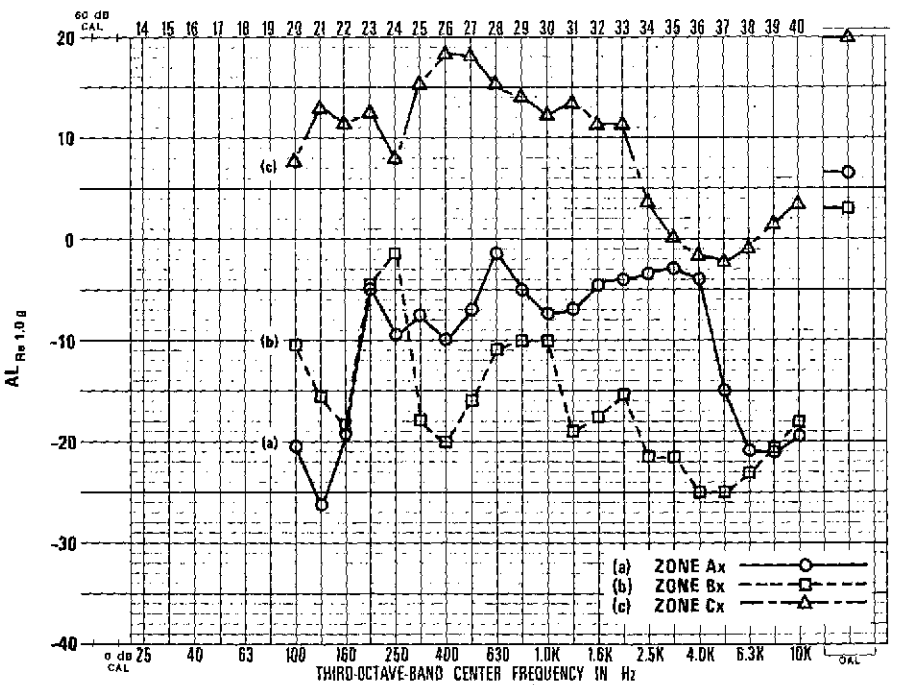

Figure 20. Baseline lateral (x-axis) acceleration response.

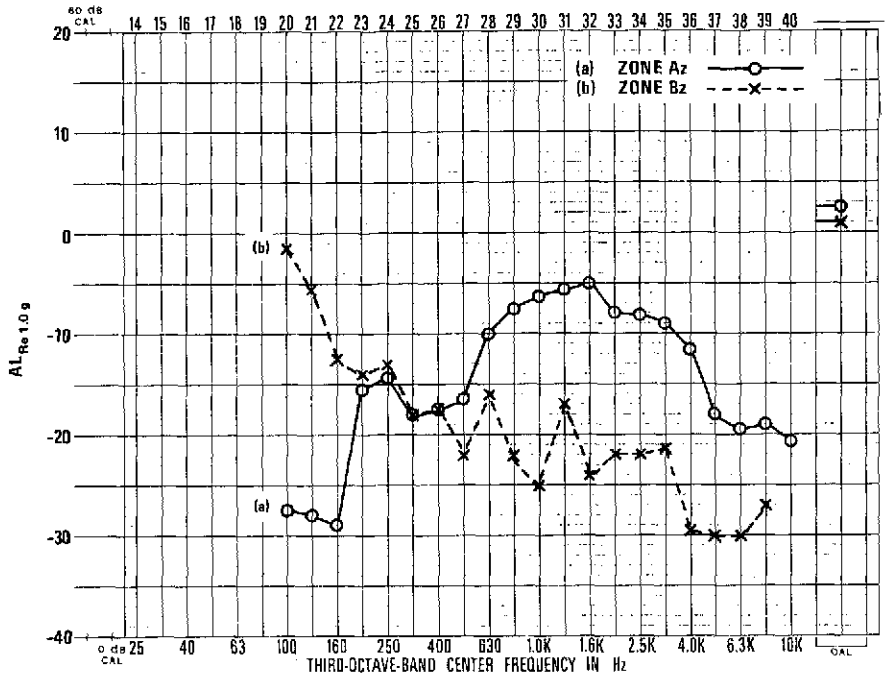

Figure 21. Baseline axial (z-axis) acceleration response.

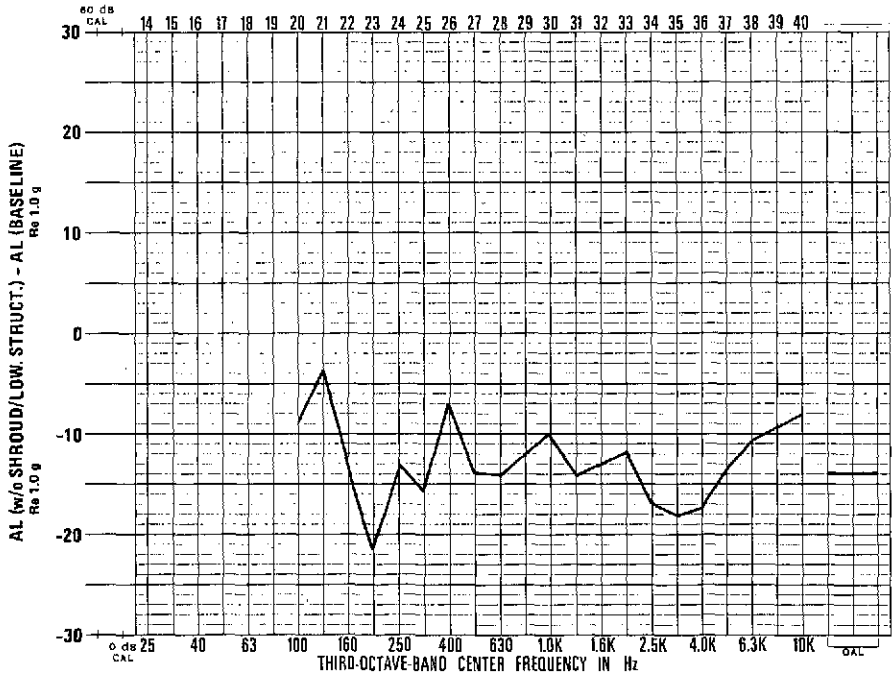

Figure 22. Zone A response generated by baseline internal SPL (without shroud and lower structure).

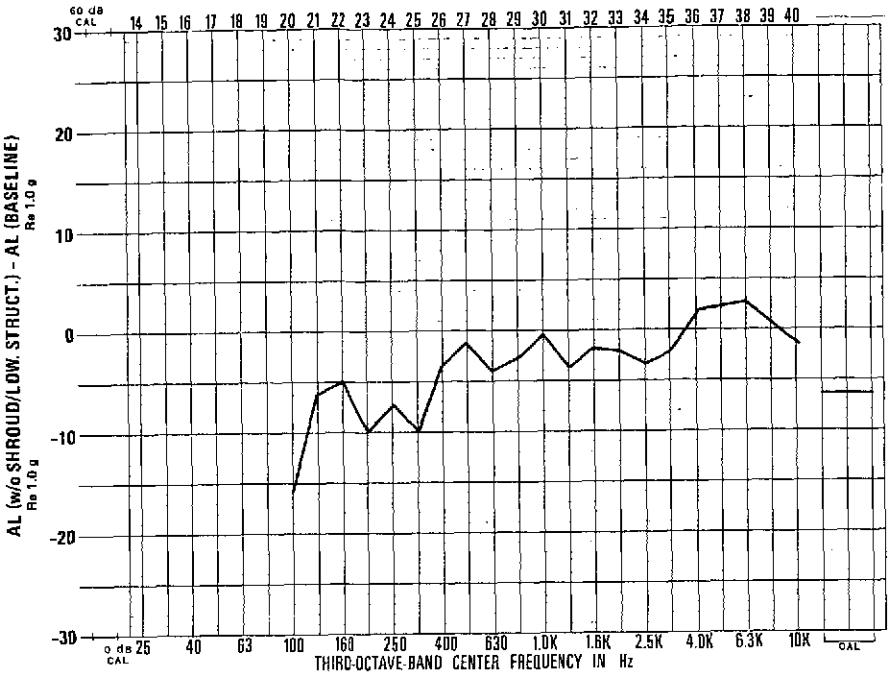

Figure 23. Zone B response generated by baseline internal SPL (without shroud and lower structure).

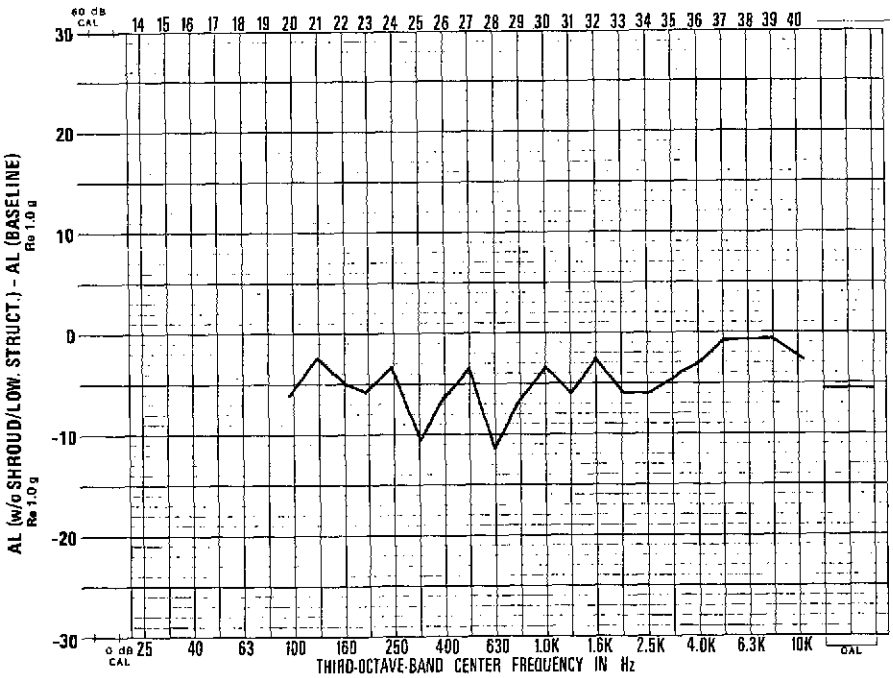

Figure 24. Zone C response generated by baseline internal SPL (without shroud and lower structure).

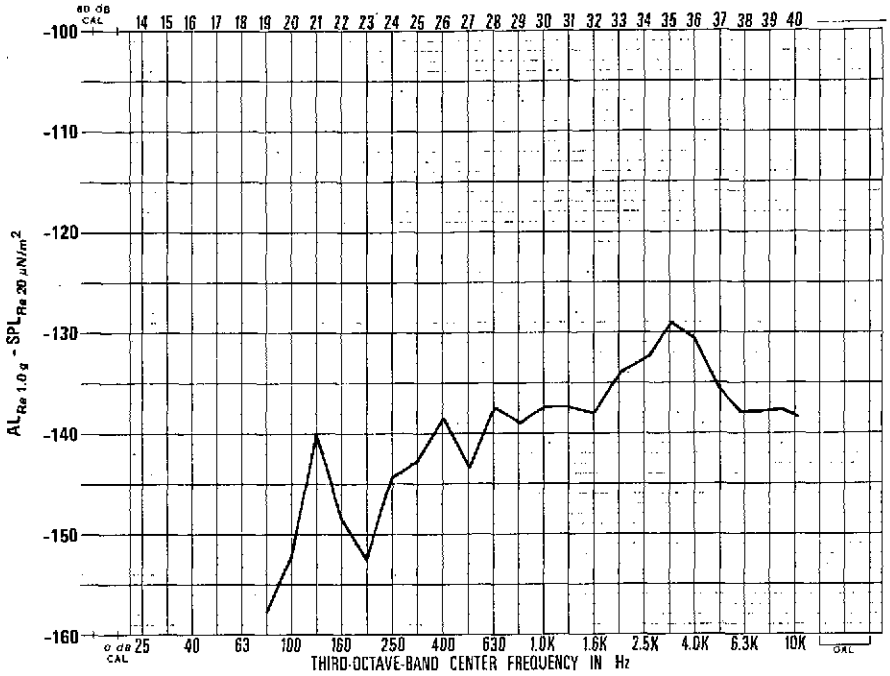

Figure 25. Transfer function for acoustic test simulation of zone A response (without shroud and lower structure).

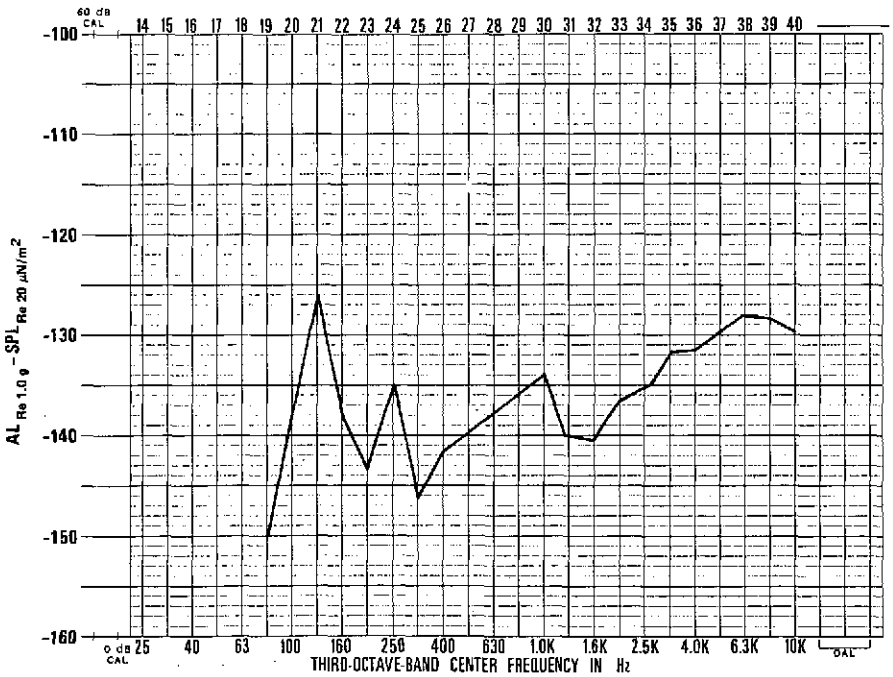

Figure 26. Transfer function for acoustic test simulation of zone B response (without shroud and lower structure).

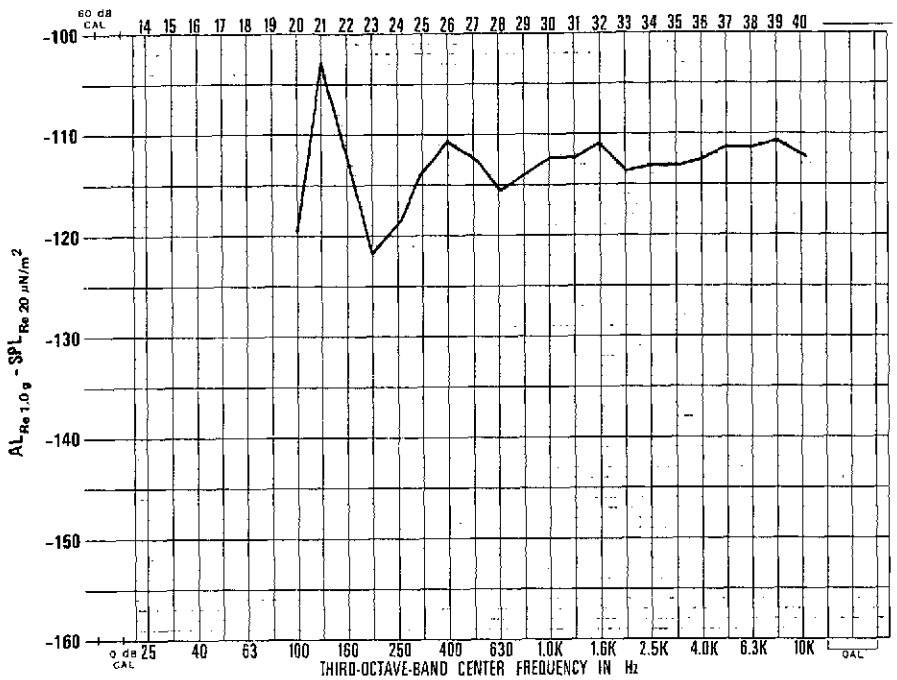

Figure 27. Transfer function for acoustic test simulation of zone C response (without shroud and lower structure).

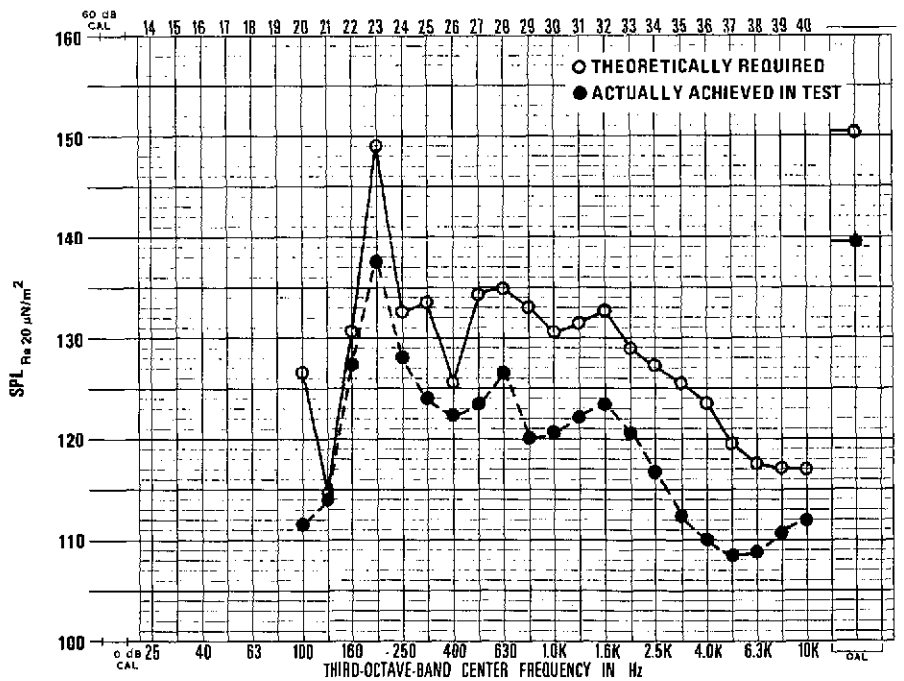

Figure 28. Acoustic input for zone A response simulation (without shroud and lower structure).

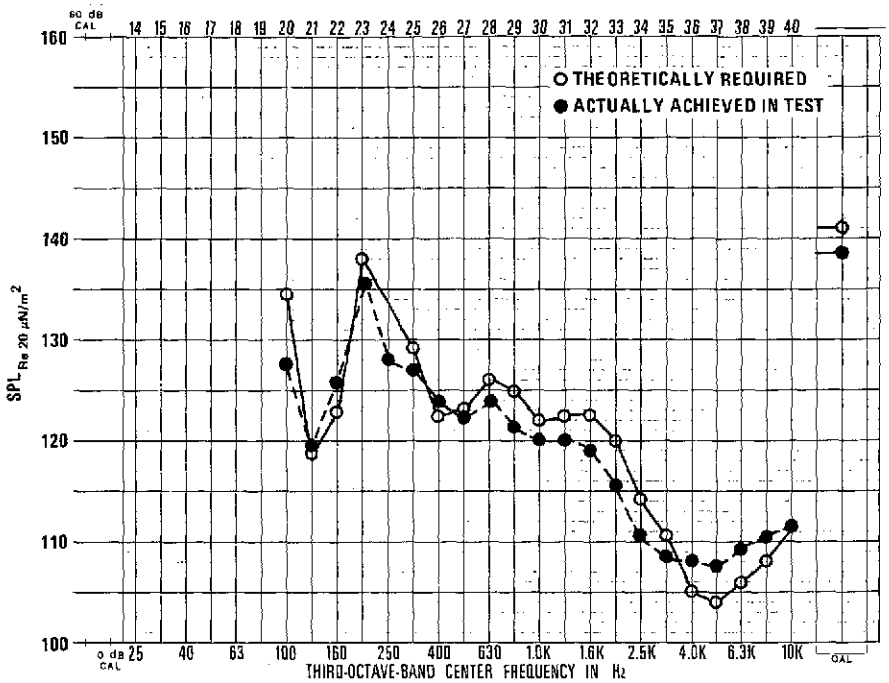

Figure 29. Acoustic input for zone B response simulation (without shroud and lower structure).

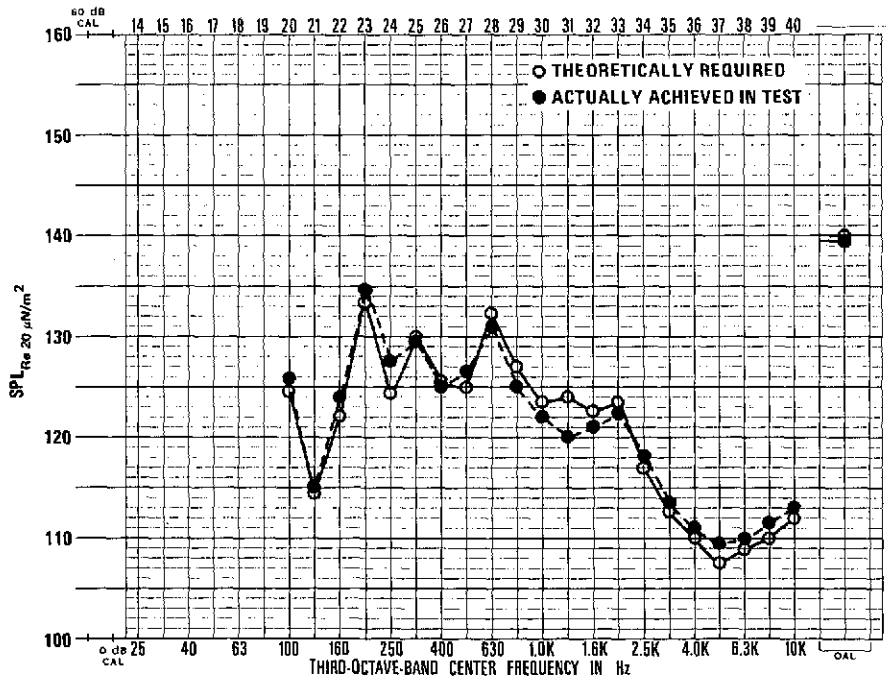

Figure 30. Acoustic input for zone C response simulation (without shroud and lower structure).

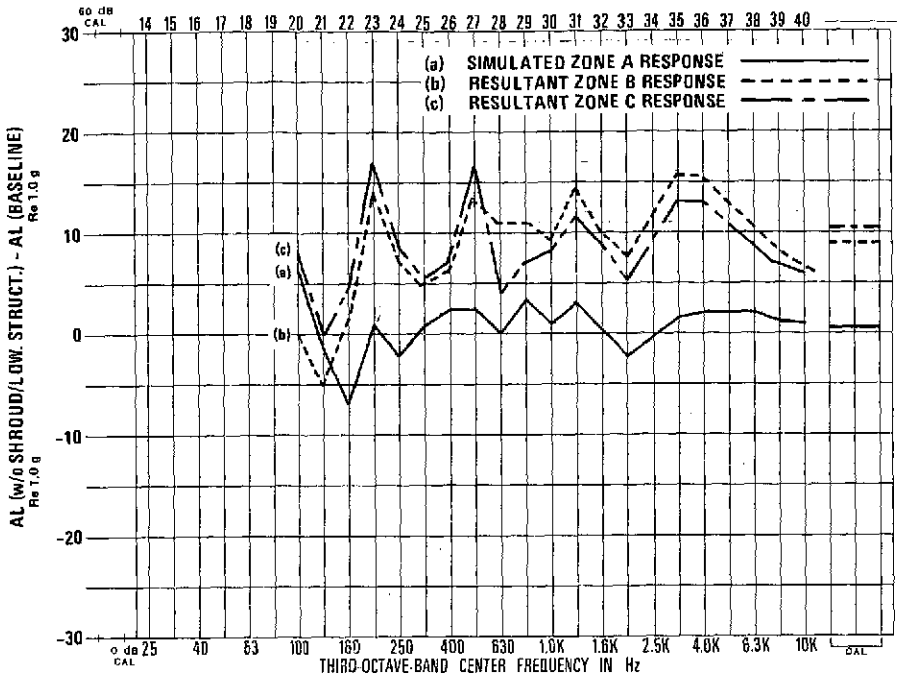

Figure 31. Zonal responses generated by figure 28 input (without shroud and lower structure) (Results are compensated for test facility limitations).

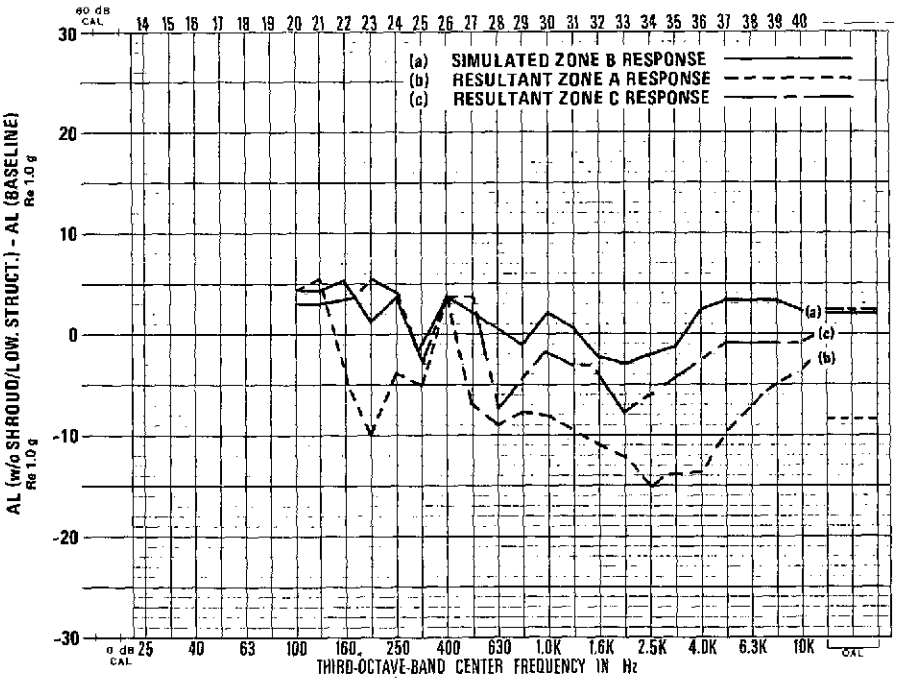

Figure 32. Zonal responses generated by figure 29 input (without shroud and lower structure).

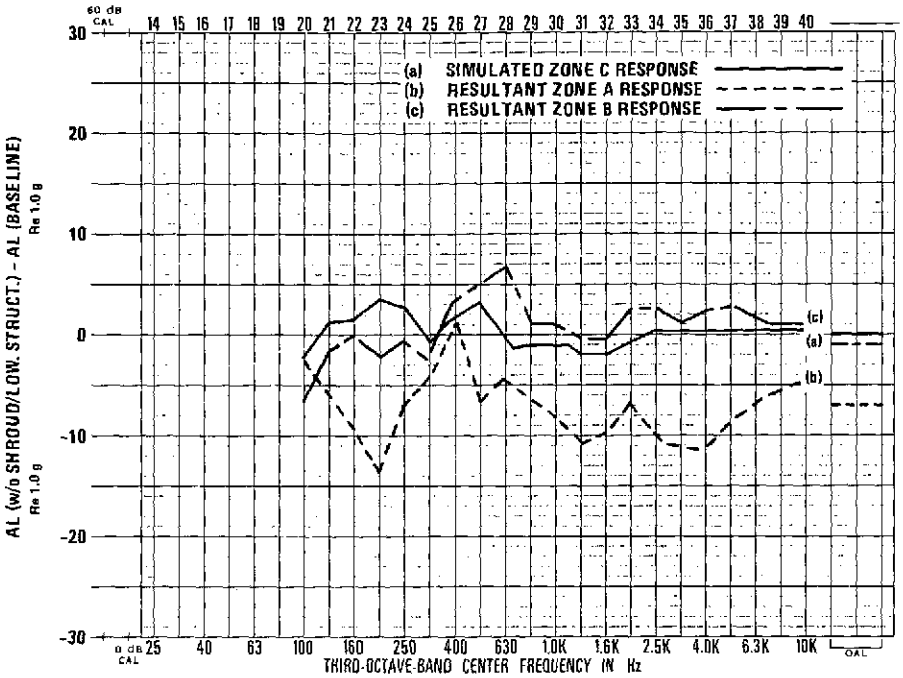

Figure 33. Zonal responses generated by figure 30 input (without shroud and lower structure).

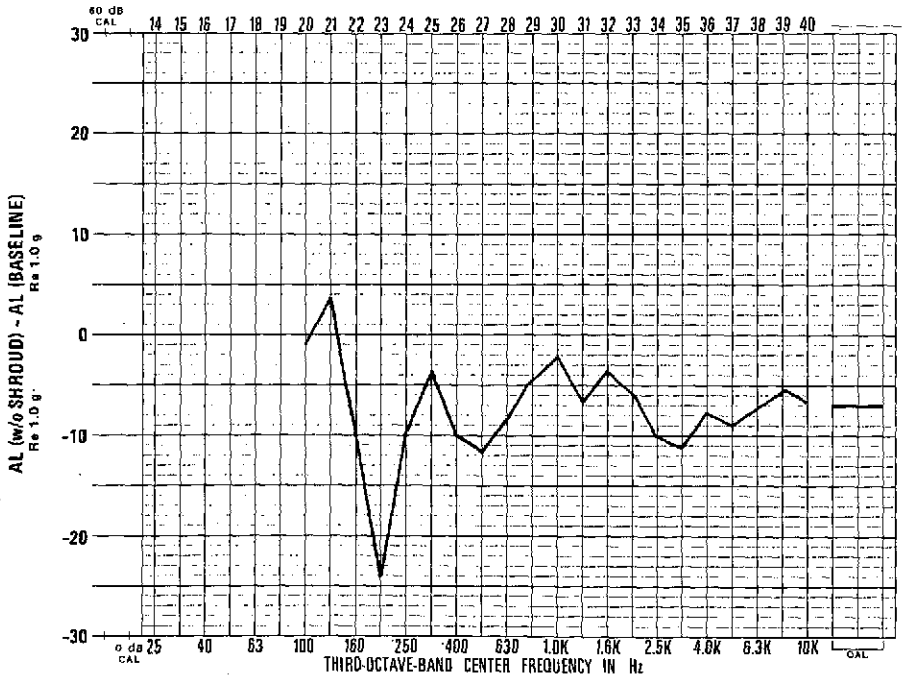

Figure 34. Zone A response generated by baseline internal SPL (without shroud).

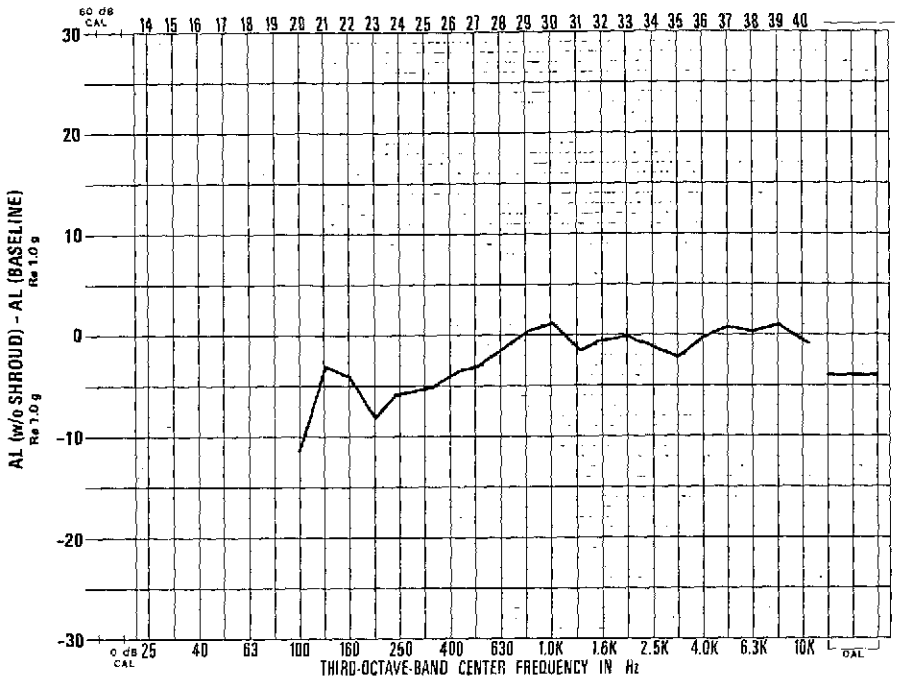

Figure 35. Zone B response generated by baseline internal SPL (without shroud).

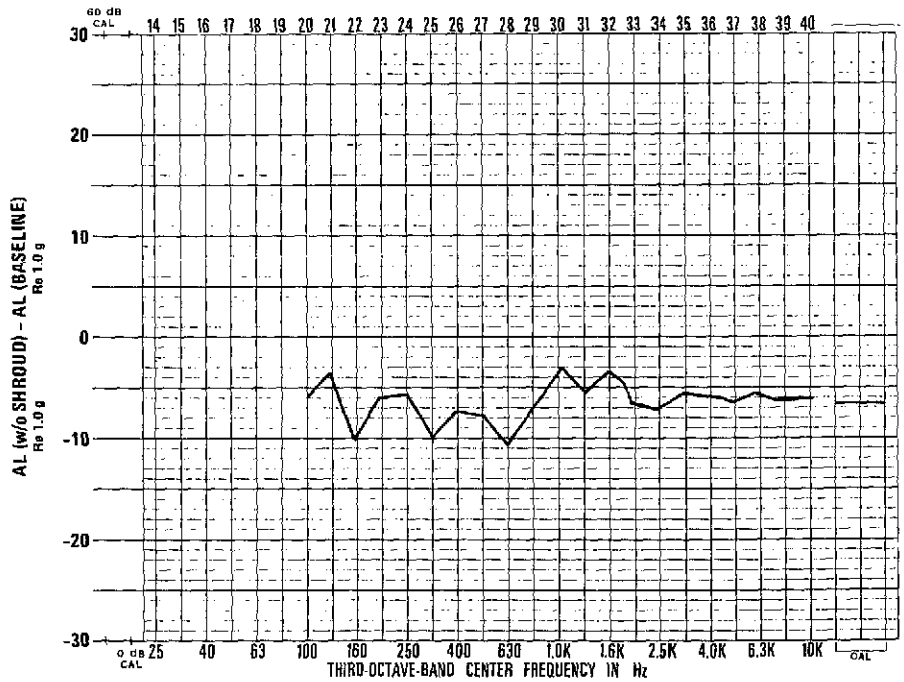

Figure 36. Zone C response generated by baseline internal SPL (without shroud).

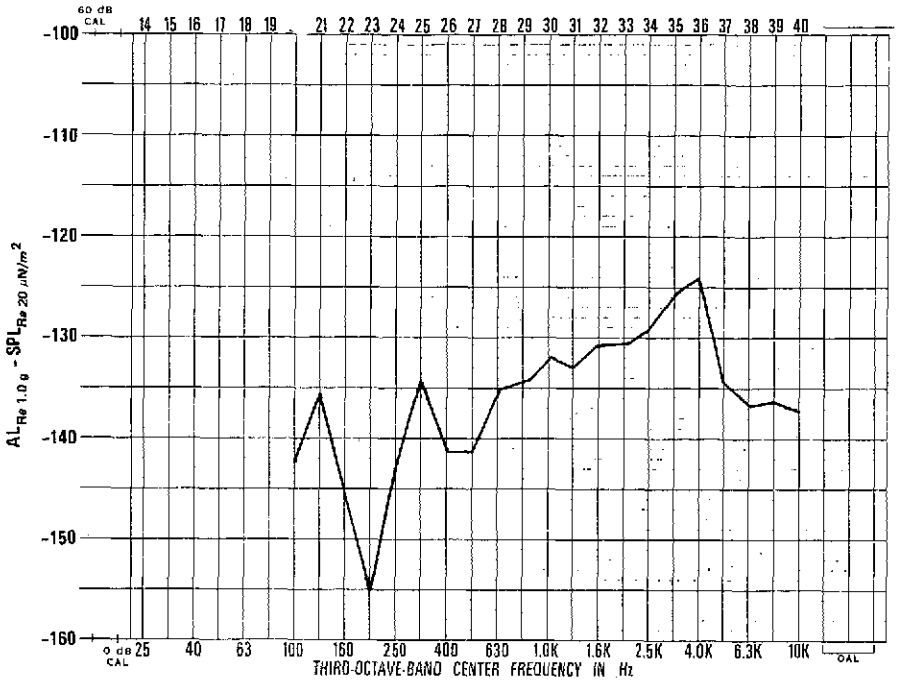

Figure 37. Transfer function for acoustic test simulation of zone A response (without shroud).

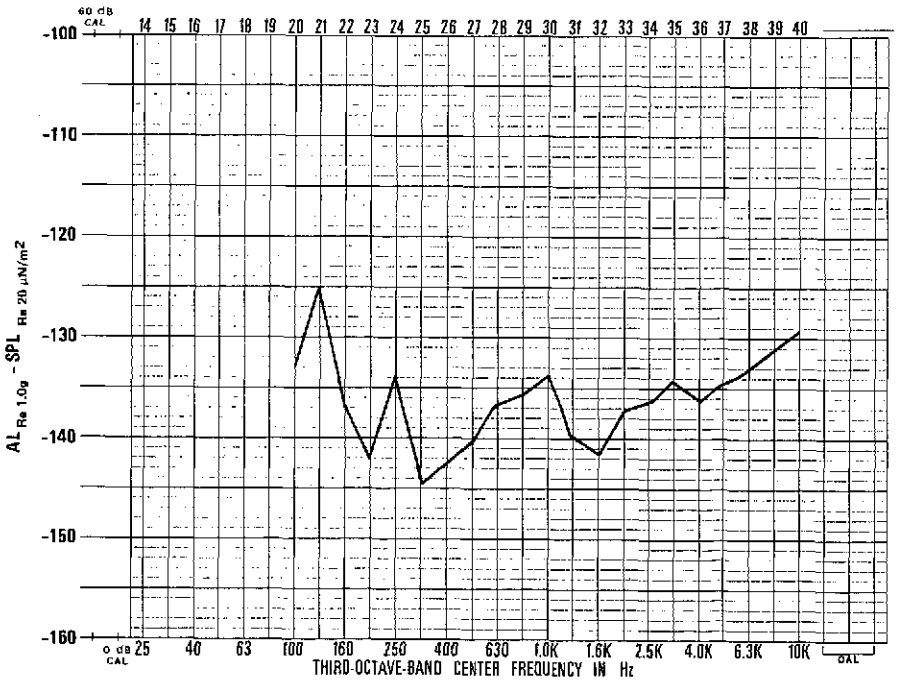

Figure 38. Transfer function for acoustic test simulation of zone B response (without shroud).

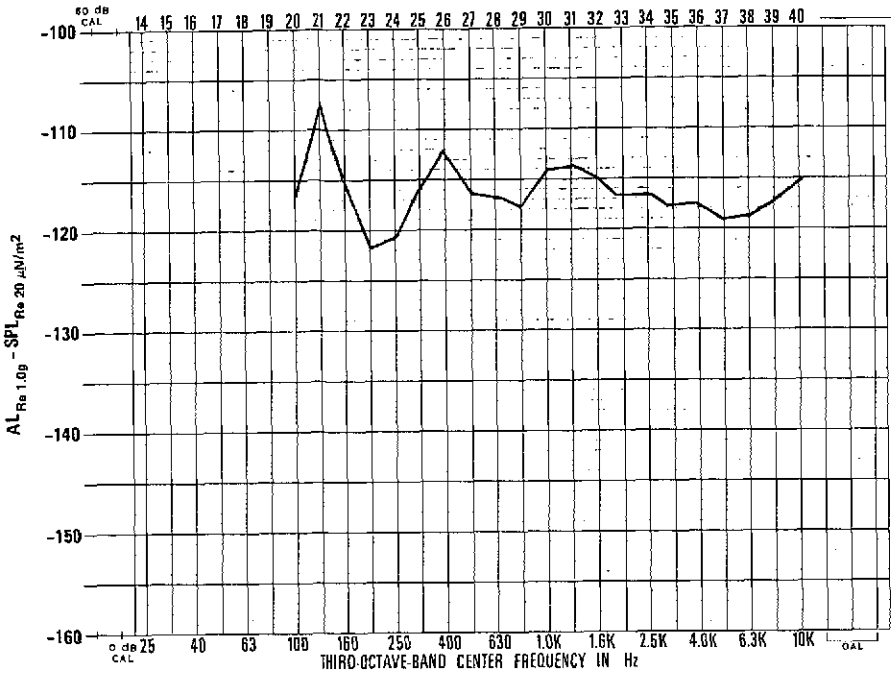

Figure 39. Transfer function for acoustic test simulation of zone C response (without shroud).

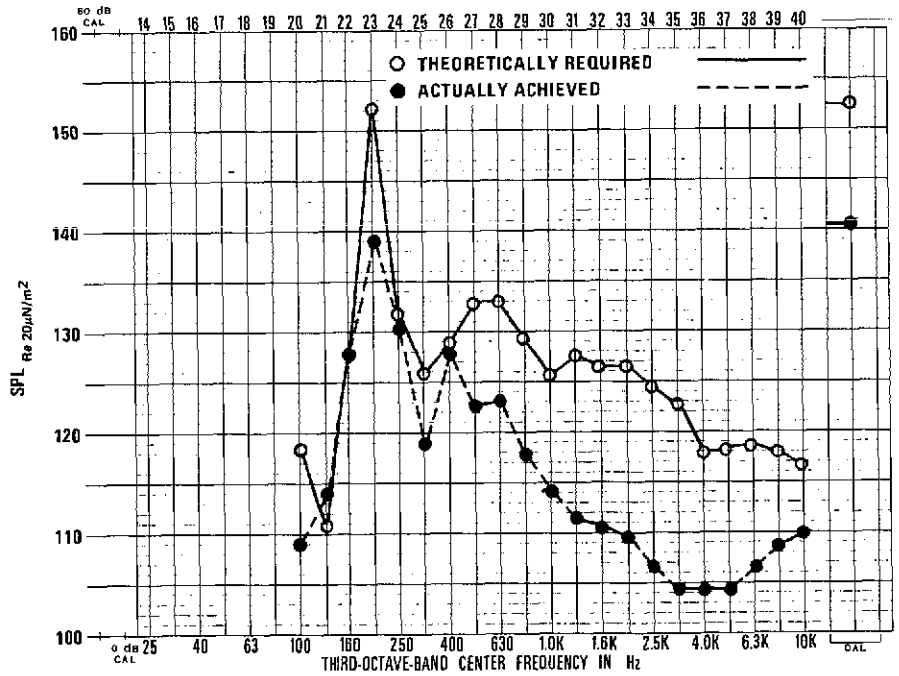

Figure 40. Acoustic input for zone A response simulation (without shroud).

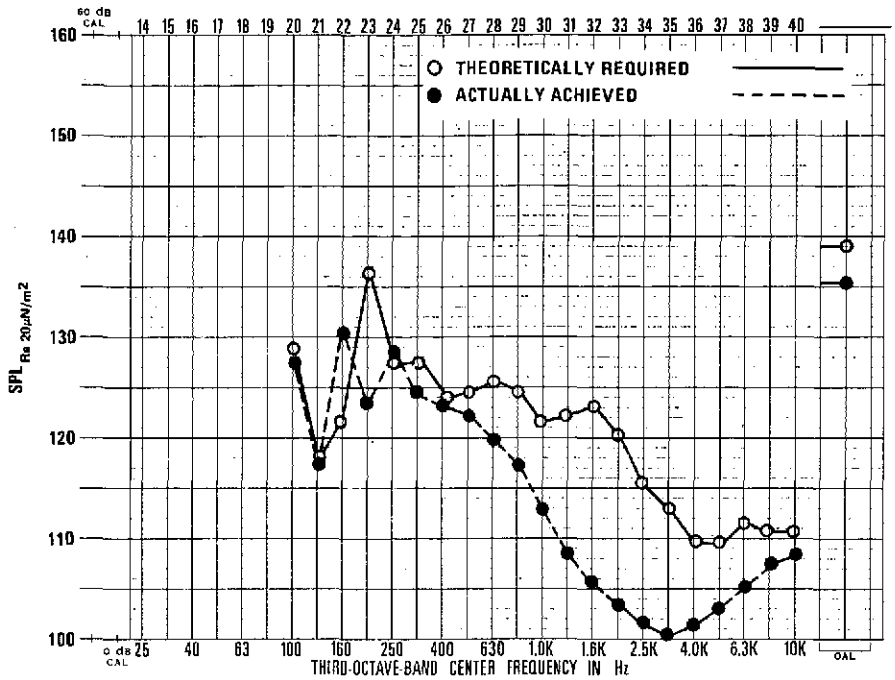

Figure 41. Acoustic input for zone B response simulation (without shroud).

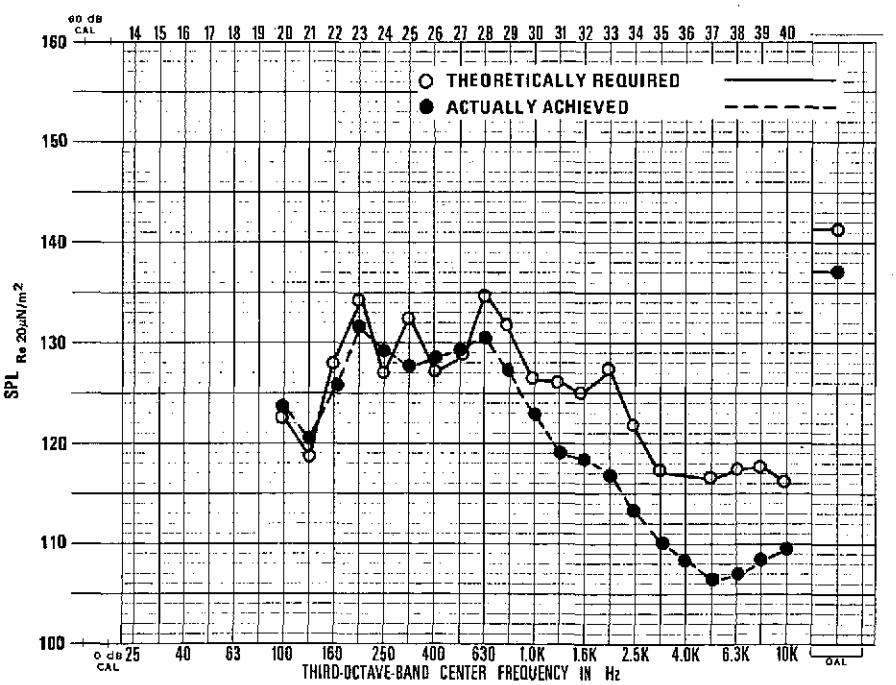

Figure 42. Acoustic input for zone C response simulation (without shroud).

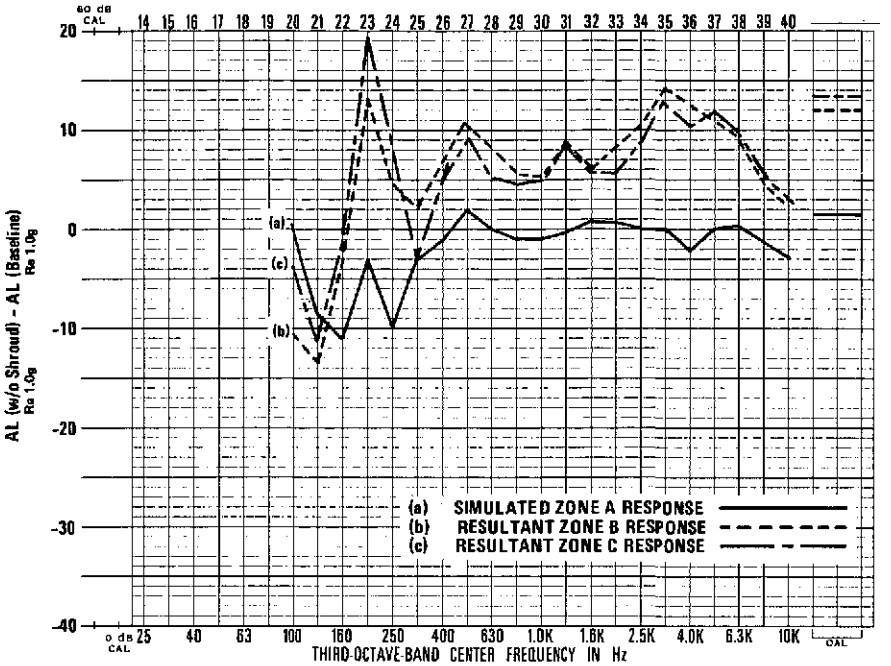

Figure 43. Zonal responses generated by figure 40 input (without shroud) (Results are compensated for test facility limitations).

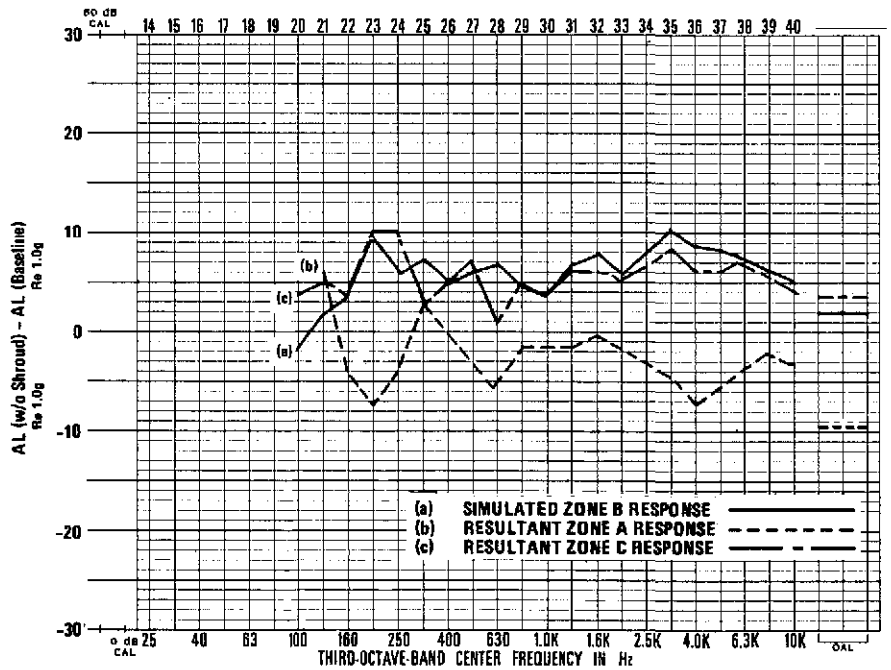

Figure 44. Zonal responses generated by figure 41 input (without shroud) (Results are compensated for test facility limitations).

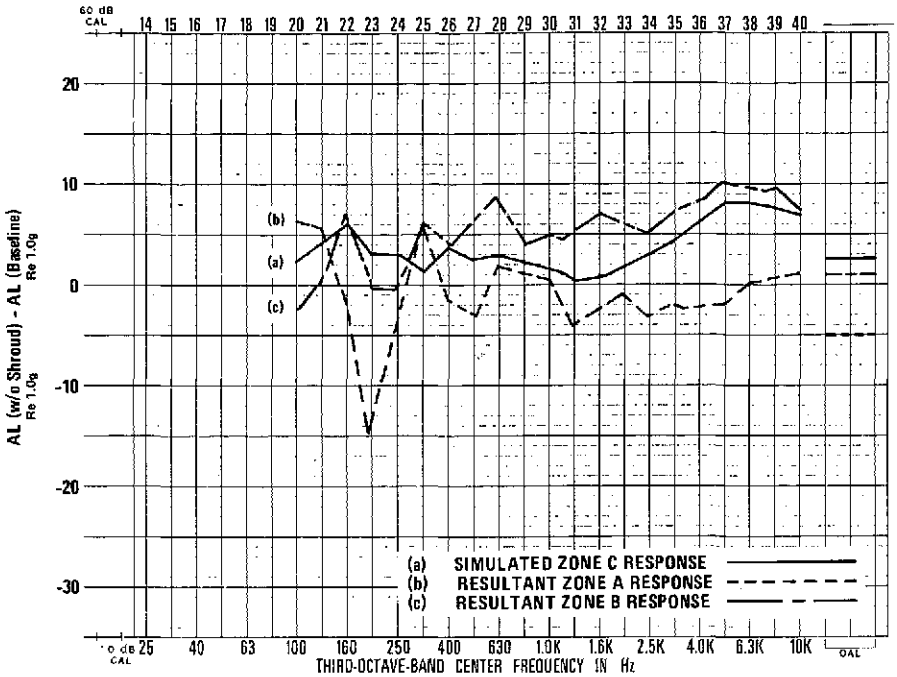

Figure 45. Zonal responses generated by figure 42 input (without shroud) (Results are compensated for test facility limitations).

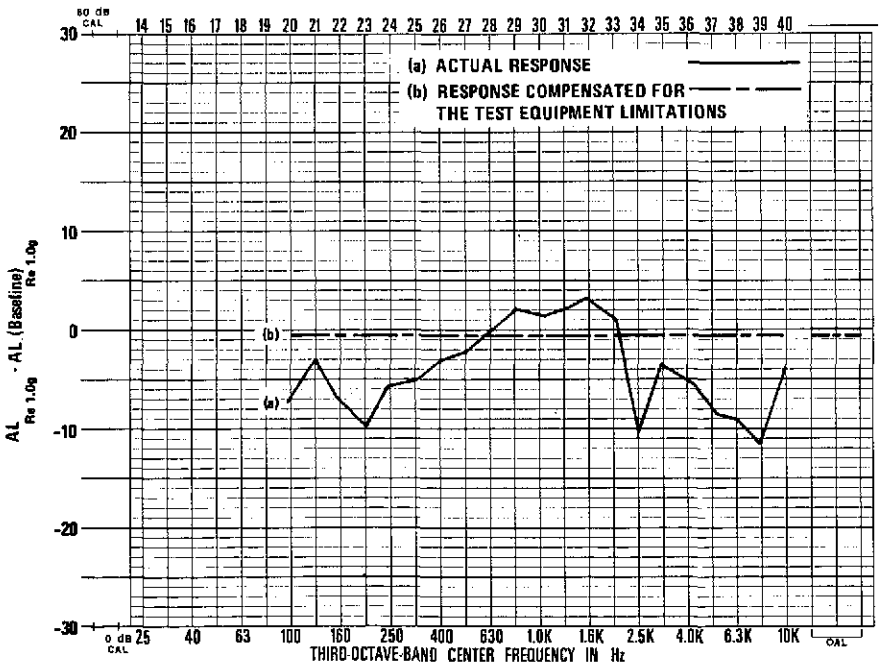

Figure 46. Zone Ax lateral response simulated by vibration test (direct servocontrolled).

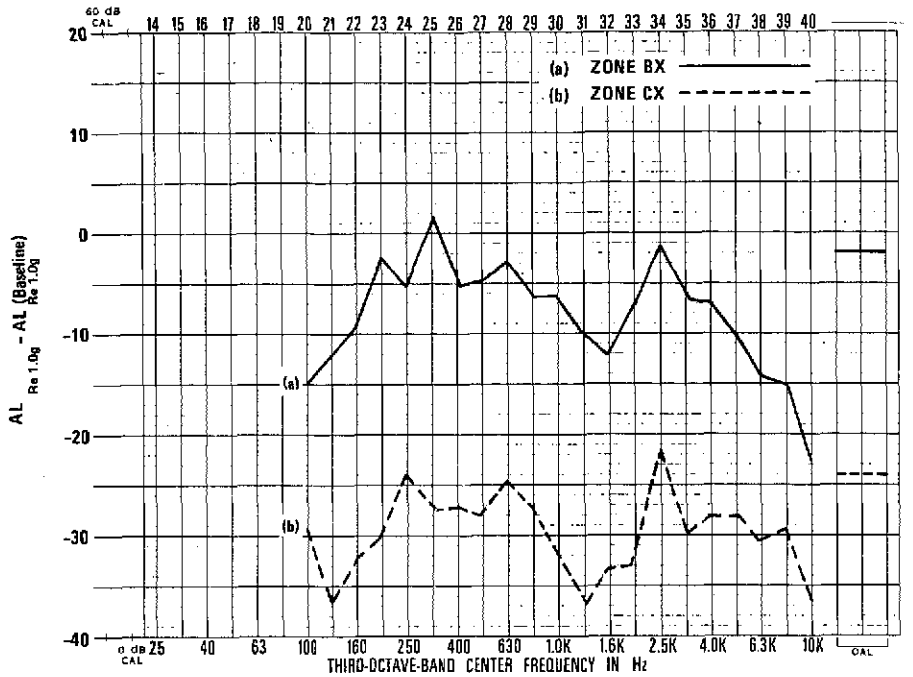

Figure 47. Resultant zone Bx and Cx lateral response generated by the zone Ax simulation of figure 46 (Results are compensated for test equipment limitations).

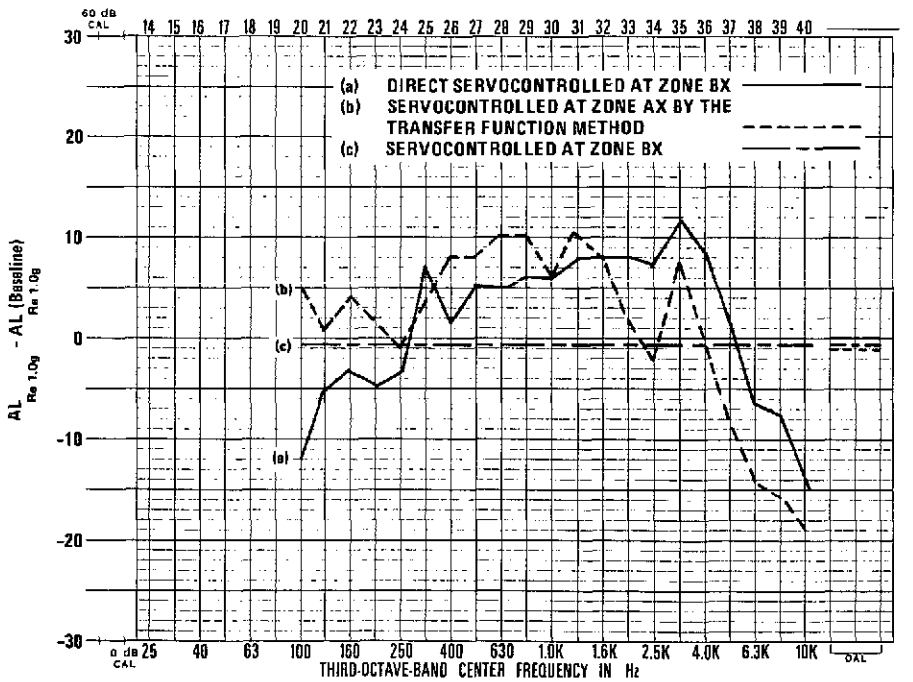

Figure 48. Zone Bx lateral response simulated by vibration test. Plot (a) is actual. On plots (b) and (c) the results are compensated for test equipment limitations.

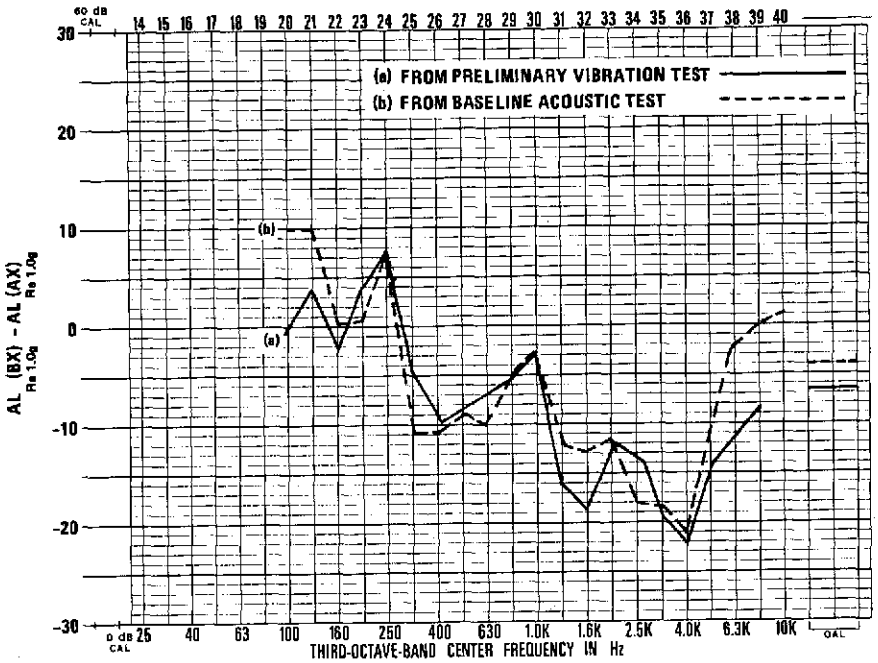

Figure 49. Transfer function for vibration test simulation of zone Bx response.

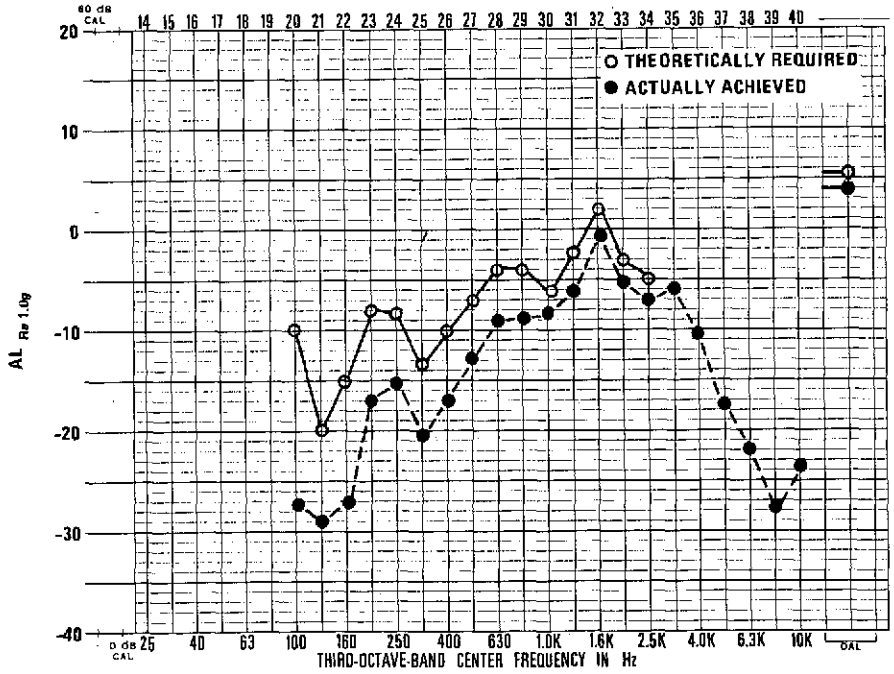

Figure 50. Vibration input at zone Ax for zone Bx response simulation.

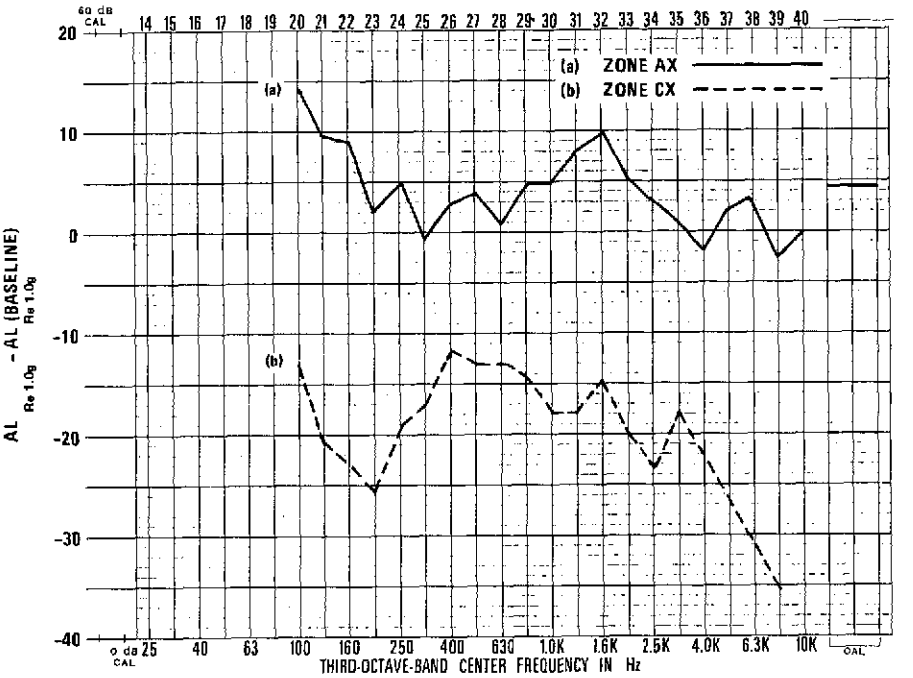

Figure 51. Resultant zone Ax and Cx response generated by vibration test simulated zone Bx response (transfer function method) (Results are compensated for test equipment limitations).

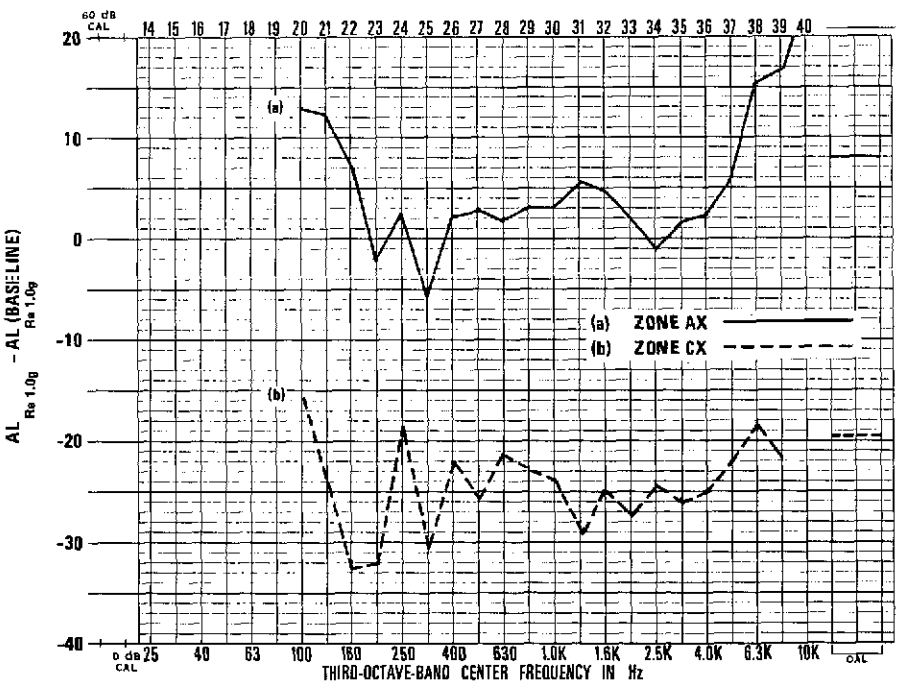

Figure 52. Resultant zone Ax and Cx response generated by vibration test simulated zone Bx response (direct servocontrolled at zone Bx) (Results are compensated for test equipment limitations).

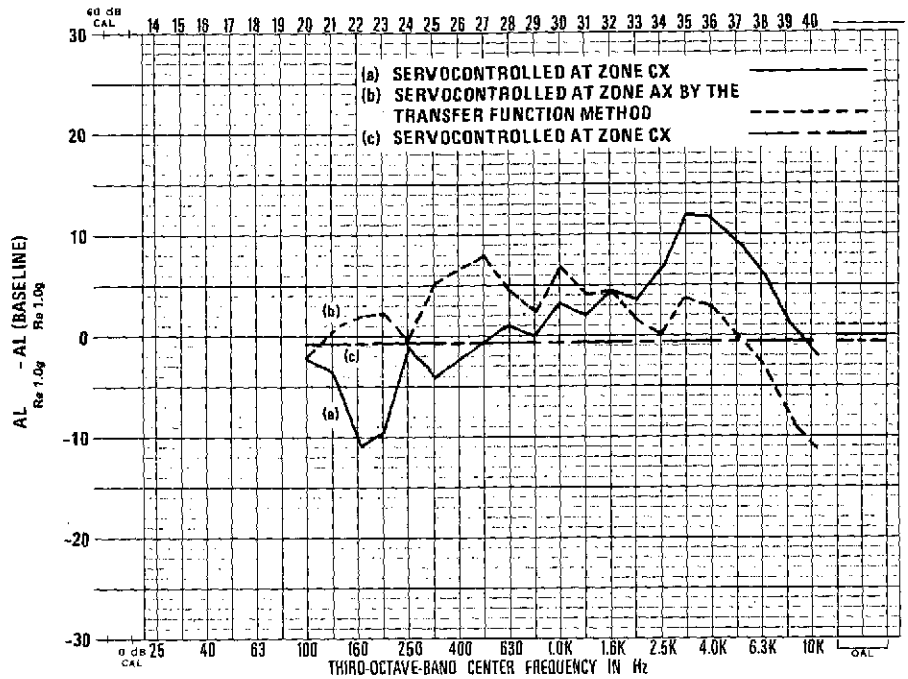

Figure 53. Zone Cx lateral response simulated by vibration test. Plot (a) is actual. On plots (b) and (c), the results are compensated for test equipment limitations.

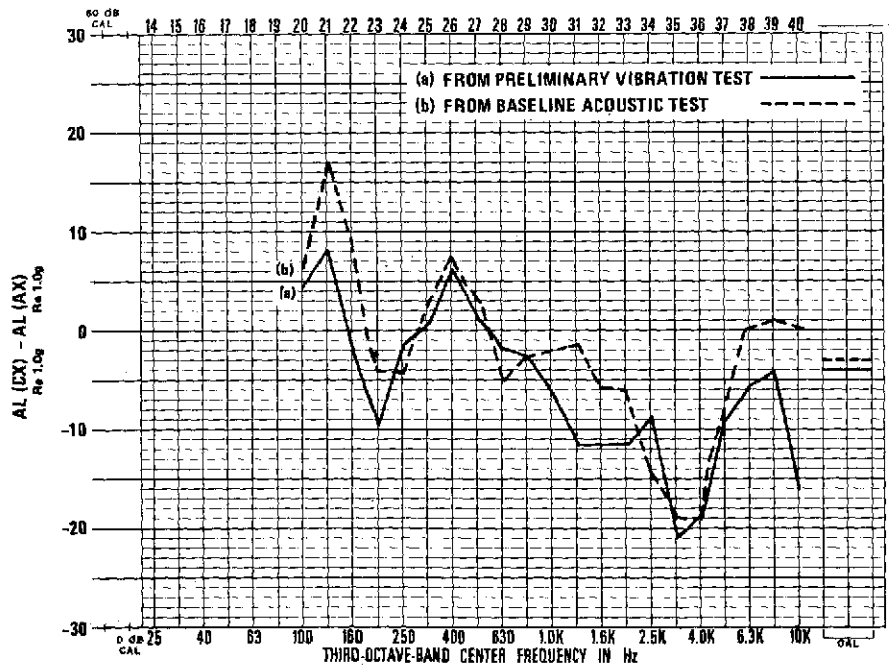

Figure 54. Transfer function for vibration test simulation of zone Cx response.

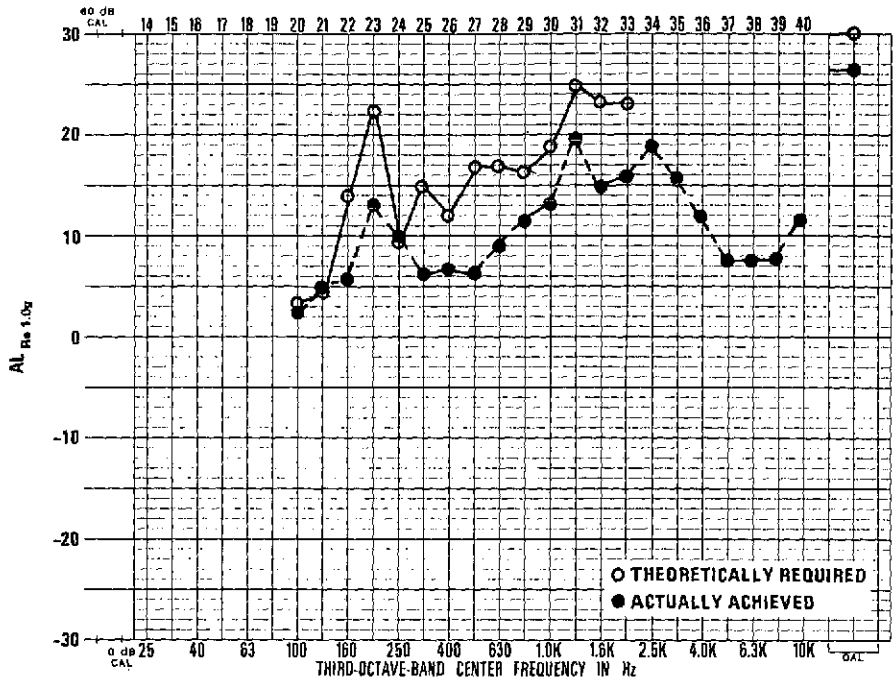

Figure 55. Vibration input at zone Ax for zone Cx response simulation.

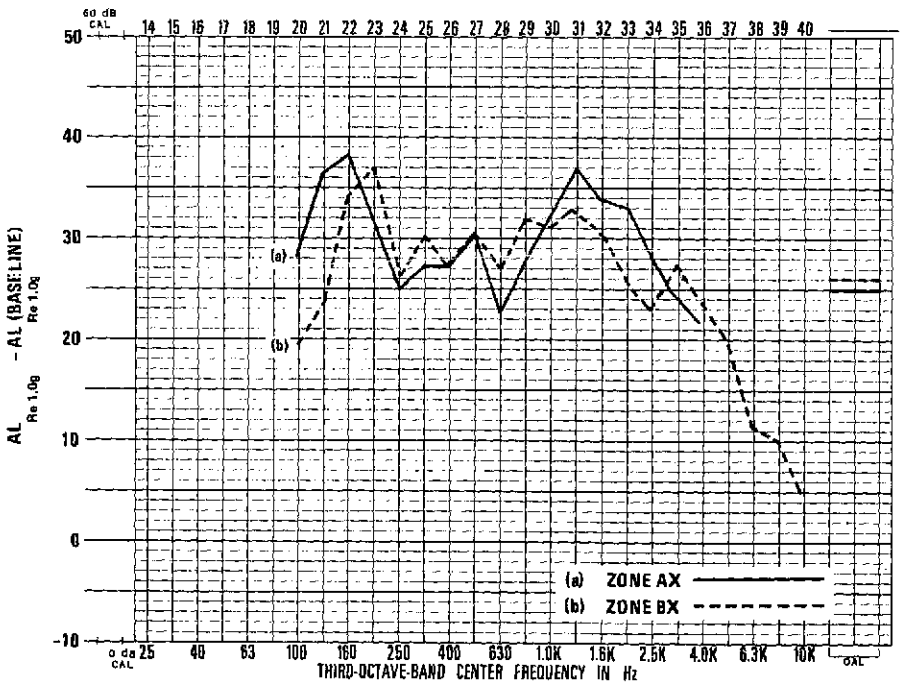

Figure 56. Resultant zone Ax and Bx response generated by vibration test simulated zone Cx response (transfer function method) (Results are compensated for test equipment limitations).

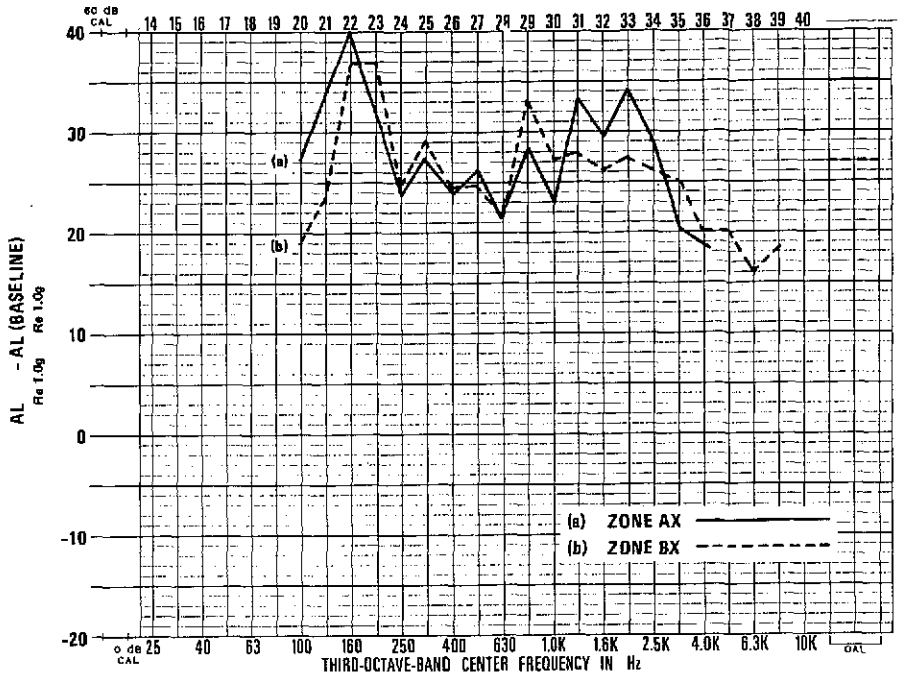

Figure 57. Resultant zone Ax and Bx response generated by vibration test simulated zone Cx response (direct servocontrolled at zone Cx) (Results are compensated for test equipment limitations).

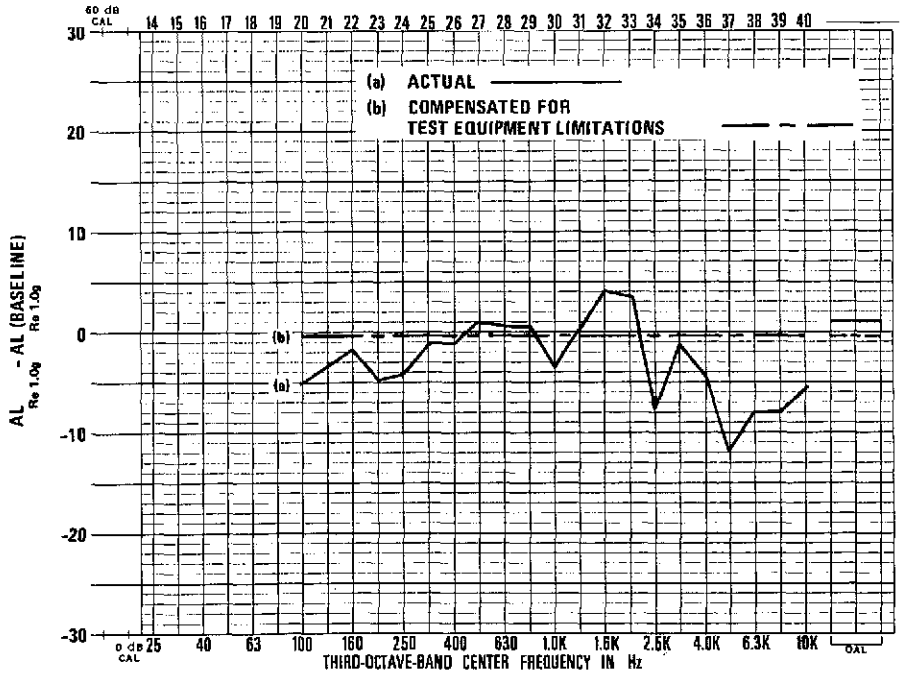

Figure 58. Zone Az axial response simulated by vibration test (direct servocontrolled).

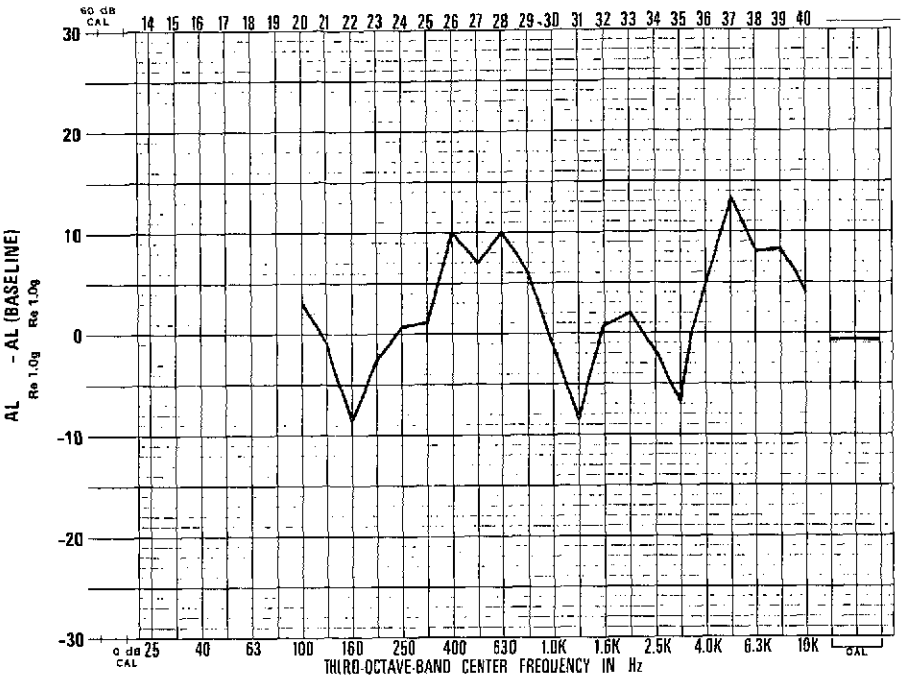

Figure 59. Resultant zone Bz response generated by vibration test simulated zone Az response (Results are compensated for test equipment limitations).

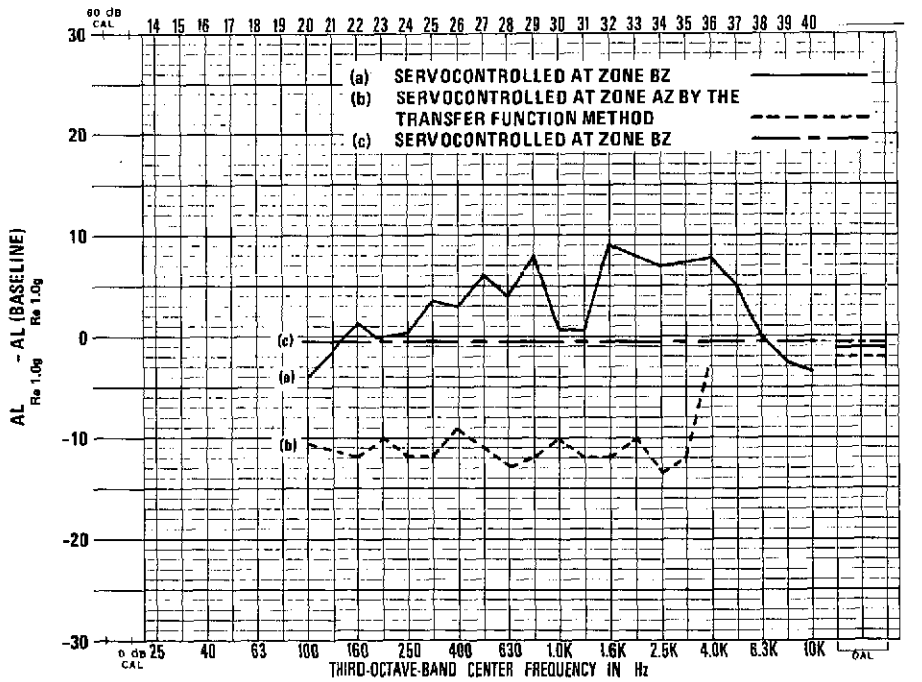

Figure 60. Zone Bz axial response simulated by vibration test. Plot (a) is actual. On plots (b) and (c), the results are compensated for test equipment limitations.

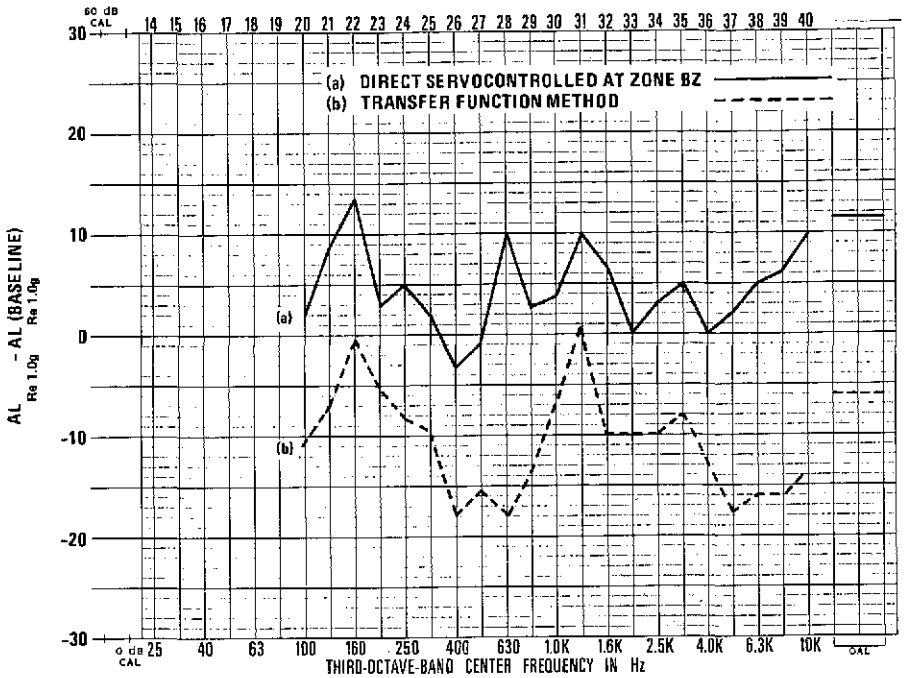

Figure 61. Resultant zone Az response generated by vibration test simulated zone Bz response (Results are compensated for test equipment limitations).

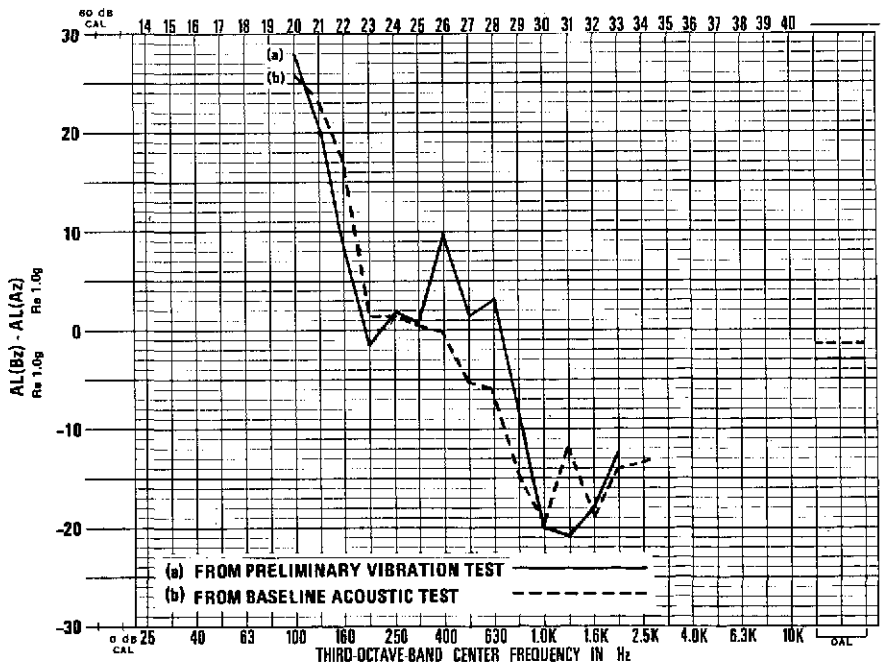

Figure 62. Transfer function for vibration test simulation of zone Bz response.

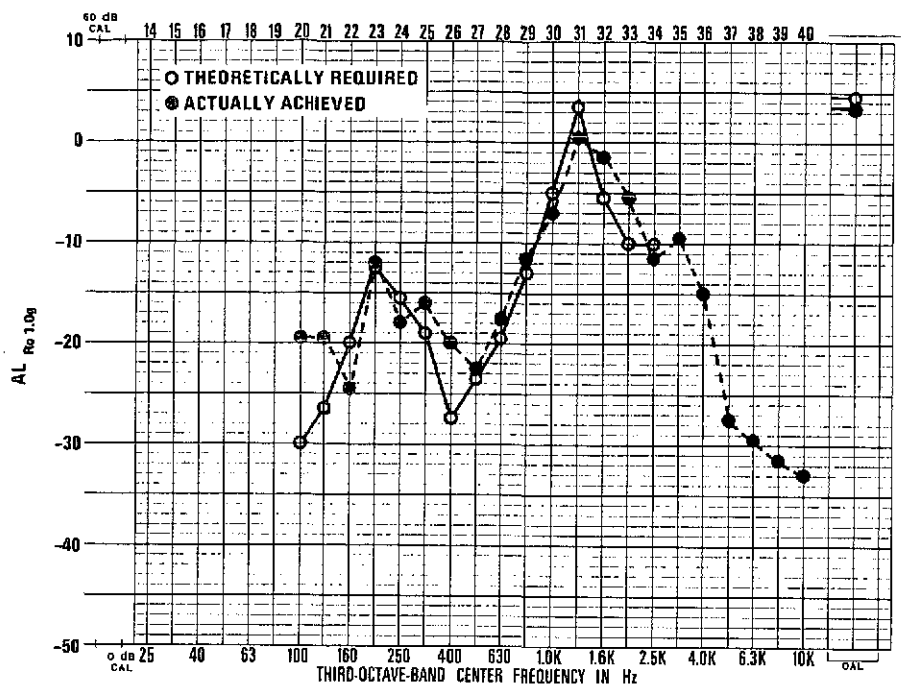

Figure 63. Vibration input at zone Az for zone Bz response simulation.

APPENDIX

SPECTRA ADJUSTMENT THROUGH THE USE OF A TRANSFER FUNCTION

This appendix summarizes a transfer function procedure for shaping the required acoustic and vibration test inputs for the spacecraft and adapter model tests.

Acoustic Test

Consider the structural response spectrum of a spacecraft resulting from a shroud-removed test (with an initial arbitrary acoustic input spectrum $P_A(f)$ to be given by A(f). Under the assumption of linear response, the equivalent acoustic input $P_E(f)$ required to generate the desired structural response D(f) of the shroud-installed spacecraft test through a shroud-removed test is determined by

$$P_E(f) = \frac{P_A(f)}{A(f)} \cdot D(f) \tag{1}$$

where $P_A(f)/A(f)$ is termed the transfer function between input and output.

In terms of sound pressure level (SPL) and response level (R), equation 1 becomes

$$SPL_E(dB) = SPL_A(dB) + R_D(dB) - R_A(dB) \tag{2}$$

where

$SPL_E = 10 \log \frac{P_E}{P_{ref}}$

$(\sqrt{P_{ref}}$ = reference pressure = 20 $\mu N/m^2$)

= equivalent SPL of acoustic input required to simulate the desired response level R_D.

$SPL_A = 10 \log \frac{P_A}{P_{ref}}$

= initial arbitrary SPL (low level)

$R_D = 10 \log \frac{D}{D_{ref}}$ ($\sqrt{D_{ref}}$ = reference response = 1.0 g rms)

= desired response level to be simulated

$R_A = 10 \log \frac{A}{A_{ref}}$ ($\sqrt{A_{ref}}$ = reference response = 1.0 g rms)

= response level generated by SPL_A.

The quantity $R_D - R_A$ thus represents the dB correction to be made to the initial without-shroud arbitrary sound pressure level (SPL_A) to give the equivalent sound pressure level (SPL_E) required to generate the desired response level R_D.

Vibration Test

For a vibration test, equation 1 becomes

$$E(f) = \frac{S(f)}{A(f)} D(f) \tag{3}$$

where

S(f)/A(f)	=	a transfer function;
E(f)	=	equivalent vibration input spectrum required to generate the desired structural response spectrum D(f);
S(f)	=	initial arbitrary (preliminary) vibration input spectrum (low level);
A(f)	=	structural response spectrum from preliminary vibration input; and
D(f)	=	desired structural response to be simulated.

In terms of input and response levels in dB units, equation 3 can be written as

$$R_E(dB) = R_S(dB) + R_D(dB) - R_A(dB) \tag{4}$$

where

$$R_E(dB) = 10 \log \frac{E}{E_{ref}} \quad (\sqrt{E_{ref}} = 1.0 \text{ g rms}).$$

SOURCES

1. Bruck, Lloyd R. *Acoustic Response Comparison for a Spacecraft Tested with and without a Shroud.* NASA TM X-65921, February 1972.

2. Cyphers, H.D., A. N. Munson, and F. J. On. *Comparative Evaluation of Predicted and Measured Performance of a 68 m^3 Reverberant Noise Chamber.* NASA TN D-7755.